NASA CR-168330

NASA

National Aeronautics and
Space Administration

AEROTHERMAL MODELING

Phase I - Final Report

Executive Summary

by
M.K. Kenworthy
S.M. Correa
D.L. Burrus

General Electric Company
Aircraft Engine Business Group
Advanced Technology Operation

Prepared for

National Aeronautics and Space Administration

NASA Lewis Research Center
Contract NAS3-23525

TABLE OF CONTENTS

I. INTRODUCTION

One of the significant ways in which the performence level of aircraft turbine engines has been improved is by the use of advanced materials and cooling concepts that allow a significant increase in turbine inlet temperature level, with attendant thermodynamic cycle benefits. Further cycle improvements have been achieved with higher pressure ratio compressors. The higher turbine inlet temperatures and compressor pressure ratios with corresponding higher temperature cooling air has created a very hostile environment for the hot section components. As a result, a major share of the engine maintenance cost is associated with the combustor and the turbine airfoils.

To provide the technology needed to reduce these hot section maintenance costs, NASA has initiated the Hot Section Technology (HOST) program. One key element of this overall program is the Aerothermal Modeling Program. The overall objective of this program is to evolve and validate improved analysis methods for use in the design of aircraft turbine engine combustors. The use of such combustor analysis capabilities can be expected to provide significant improvement in the life and durability characteristics of both combustor and turbine components. Another expected benefit is a significant reduction in expensive combustor development testing and the associated costs.

II. OBJECTIVE

The objective of Phase One of the Aerothermal Modeling Program was to identify deficiencies in the aerothermal models that are currently used or planned for use at General Electric in the design of gas turbine engine combustors. This effort was accomplished by assessing the predictions of existing models with benchmark quality test data. This effort, together with other similar efforts sponsored by NASA, was intended to assess the current state of the art. It was also intended to define Phase Two efforts needed to evolve improved and more advanced aerothermal analysis methods,--thereby enhancing available capabilities for the design of high performance and durable combustors for advanced aircraft turbine engines.

This Phase I effort was focused on the ability of the existing models to predict or analyze those features associated with durability. These primarily are (1) the combustor liner metal temperature distribution, and (2) the combustor exit gas temperature patterns, which in turn affects the life of the downstream turbine components. Other features of interest to the combustor designer, such as blowout limits and pollutant emission levels, do not directly affect design for durability.

III. THE GENERAL ELECTRIC AEROTHERMAL MODEL

Figure 1 shows schematically General Electric's calculation modules within the overall aerothermal model. Except for the internal flow module, the modules are well developed and have been in use for many years. The internal flow module is planned for use in the design process at General Electric after it has been developed and/or demonstrated to have useful accuracy. Thus, the assessment of the candidate internal flow modules, available at General Electric, constituted a major portion of the efforts reported herein.

Briefly the modules shown in Figure 1 provide the following calculated results. The Preliminary Design Module provides the basic features of the combustor, including its flowpath and the number of fuel nozzles, early in the design process. The Diffuser Module calculates diffuser pressure losses and the three individual pressure levels that feed the inner and outer flow path, and the dome region. The Flow Distribution Module, using the diffuser exit pressure levels, total airflow, fuel flow, and the combustor aperture areas and features, calculates the flow and flow angle through each aperture, as well as a one-dimensional internal gas temperature and the overall pressure drop. The program has features to determine effective flow areas from the particular aperature shape and approach flow velocity. A large effective flow area data base exists at General Electric, and new measurements are made on individual apertures whenever needed. The Heat Transfer Module is used to calculate metal temperatures throughout the combustor structure via conventional heat transfer equations, together with correlations of cooling film effectiveness based on wind tunnel data. It utilizes the flow distribution, including liner cooling slot flows; the velocities on the cold side of the liner, along with assumed profiles for the one dimensional internal gas temperatures; and velocities from the Flow Distribution Module. This information, together with aerodynamic pressure loading from the Flow Distribution Module, is then used as input to stress and life analysis procedures to provide life estimates or to indicate the life effects of a postulated design change. The Internal Flow Module calculates detailed three-dimensional (3-D) temperature and velocity patterns throughout the combustor flow field. The three submodules indicated reflect different aspects of the internal flow modeling, but all are treated with the same basic 3-D elliptical calculation framework. An accurate 3-D elliptic computer code could provide substantially better hot gas side inputs to the Heat Transfer Module than the present method. Also, the Internal Flow Module provides an analytical calculation of the detailed exit gas temperature pattern for use by the turbine designer in calculating metal temperature distributions, stresses, and life.

Metal temperatures are, of course, measured on combustors, but in only a finite number of places. The available stress and life analysis procedures need more than isolated temperature measurements. They need the detailed temperature distribution provided by the Heat Transfer Module. Figure 2 illustrates a heat transfer module axial node pattern for a single panel of a combustor. Circumferential effects are also needed. The major source of error in the Heat Transfer Module is in the estimation of the inputs on the

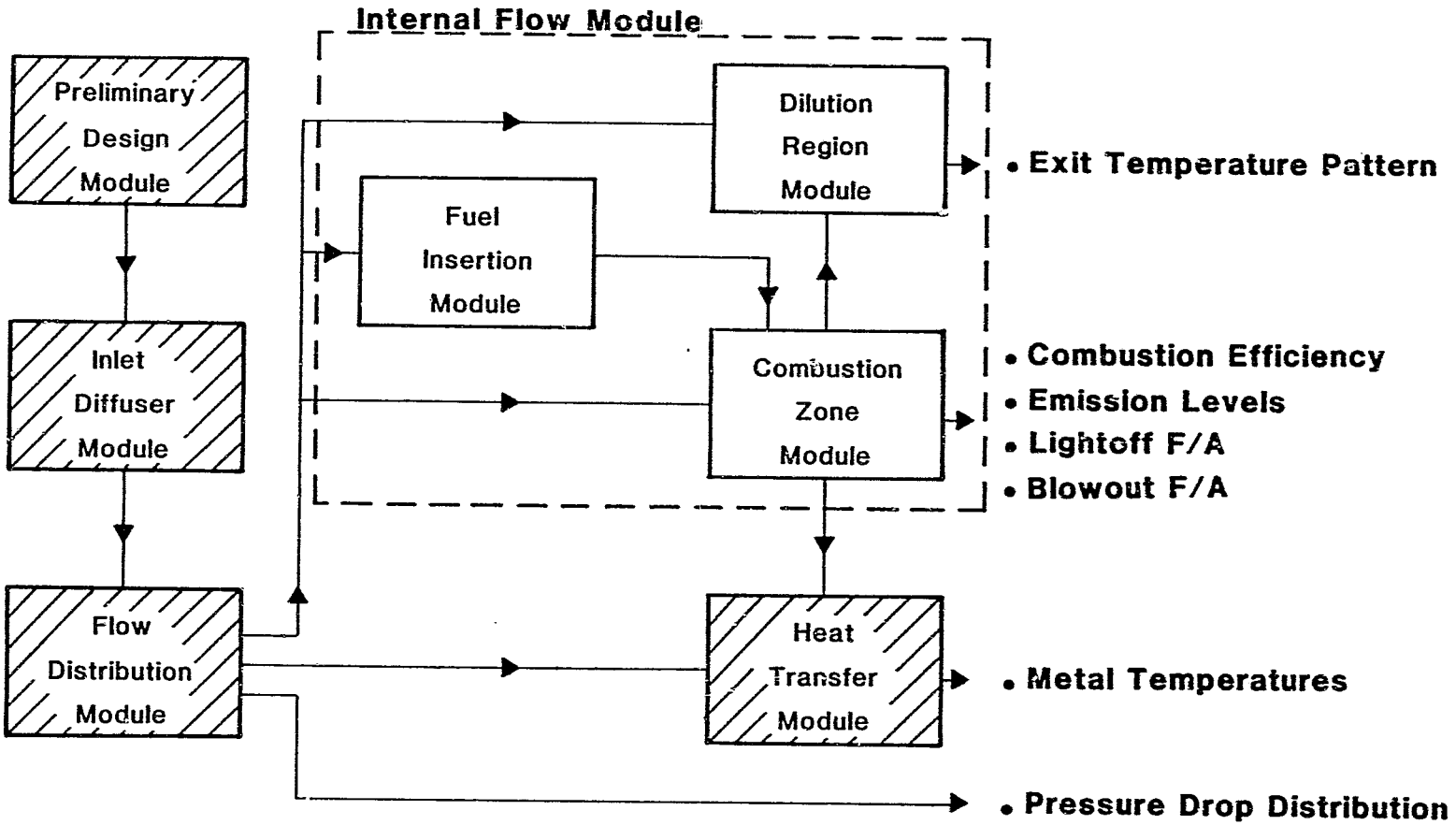

- **Shaded boxes are modules in current use in combustor design and development work.**
- **Open boxes are modules in General Electric's aerothermal model planned for use in the future in design and development work after adequate accuracy is demonstrated or developed.**

Figure 1. Flow Diagram of Overall General Electric Aerothermal Model.

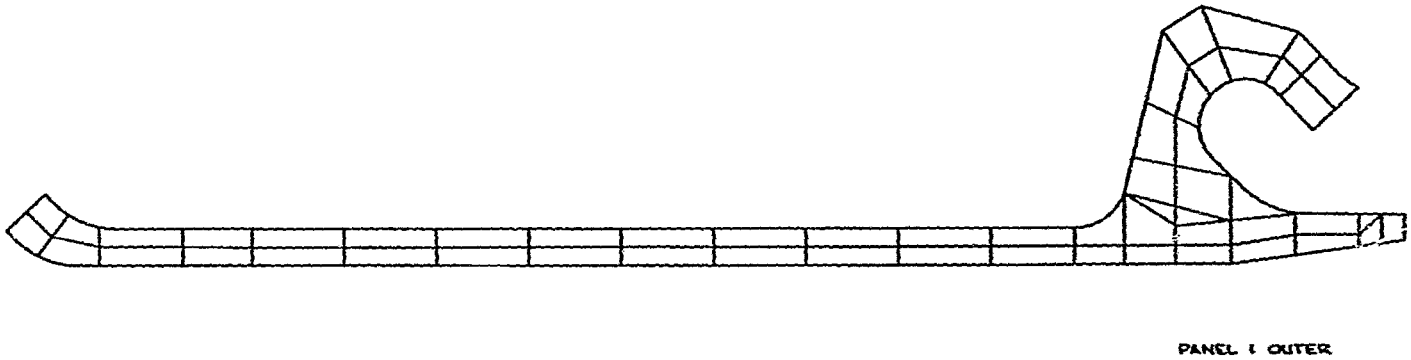

Figure 2. Typical Node Pattern for Liner Heat Transfer Calculations.

hot gas side - the local flow velocities, gas temperatures, and flame radiation levels. An accurate 3-D elliptic computer code for calculating the internal flow field could provide substantially better inputs.

At General Electric, combustor exit gas temperature patterns are measured in detail, typically at seven radial positions and every 1-1/2 degrees around the circumference. This information is adequate in detail for the turbine designers. However, improving or modifying temperature pattern during the development of the combustor usually involves many cut-and-try test efforts. Changes are often defined with the help of existing data or correlations of simple jet penetration experiments in a cross flow, or measurements of flows emerging from the swirl cups surrounding a fuel nozzle in a simple bench experiment. An accurate internal flow module would be very valuable in providing more detailed and precise inputs and, thus, in reducing total development tests.

Two basic codes for calculating 3-D elliptic reacting flows are available at General Electric and included in the structure of INTFLOW: (1) The code assembled by the Garrett Turbine Company under the Army-sponsored Combustor Design Validation Program efforts, Reference 1; and (2) the very similar code assembled by the Northern Research and Engineering Company, Reference 2. In addition, two 2-D codes are available: (1) The TEACH code developed initially at Imperial College which uses essentially the same methods as the previous two codes but in a 2-D instead of 3-D framework; and (2) the two-dimensional (planar or axisymmetric) research code, GETREF (General Electric Turbulent Reacting Flow) developed at General Electric. The 2-D GETREF code provided a valuable addition to the 3-D codes because its physical submodels and numerical techniques are more rigorous. Figure 3 is an illustration of a calculation from the GETREF code dealing with the initial swirl cup portion of a combustor where the flows are initially axisymmetric.

Prior to this Phase I effort, plotting routines for the output and some improved flexibility for input had been coupled at General Electric with the 3-D elliptic codes. This new format, containing both the Garrett and the Northern Research 3-D codes, was defined as the INTFLOW program. Programming improvements were not to be part of the scope on this Phase I effort. For a typical full annular combustor, a 3-D model of a segment containing one fuel nozzle is modeled. Figure 4 illustrates a calculated flow field obtained from the 3-D INTFLOW program. The length of the arrows are proportional to the calculated velocities. Only recently have computer storage capabilities been able to accept a model with this much grid detail, see Figure 5. Little additional grid detail can be introduced at this time due to computer storage limits, but the cost of obtaining a converged solution with more grid could become too great at present computer running time costs.

Some of the immediately obvious limitations of the existing 3-D internal flow codes that were recognized at the outset and influenced the assessments conducted in Phase I were, as follows:

1. With the grid shown in Figure 5 the so called "hybrid" numerics in the program involve the introduction of significant artificial or

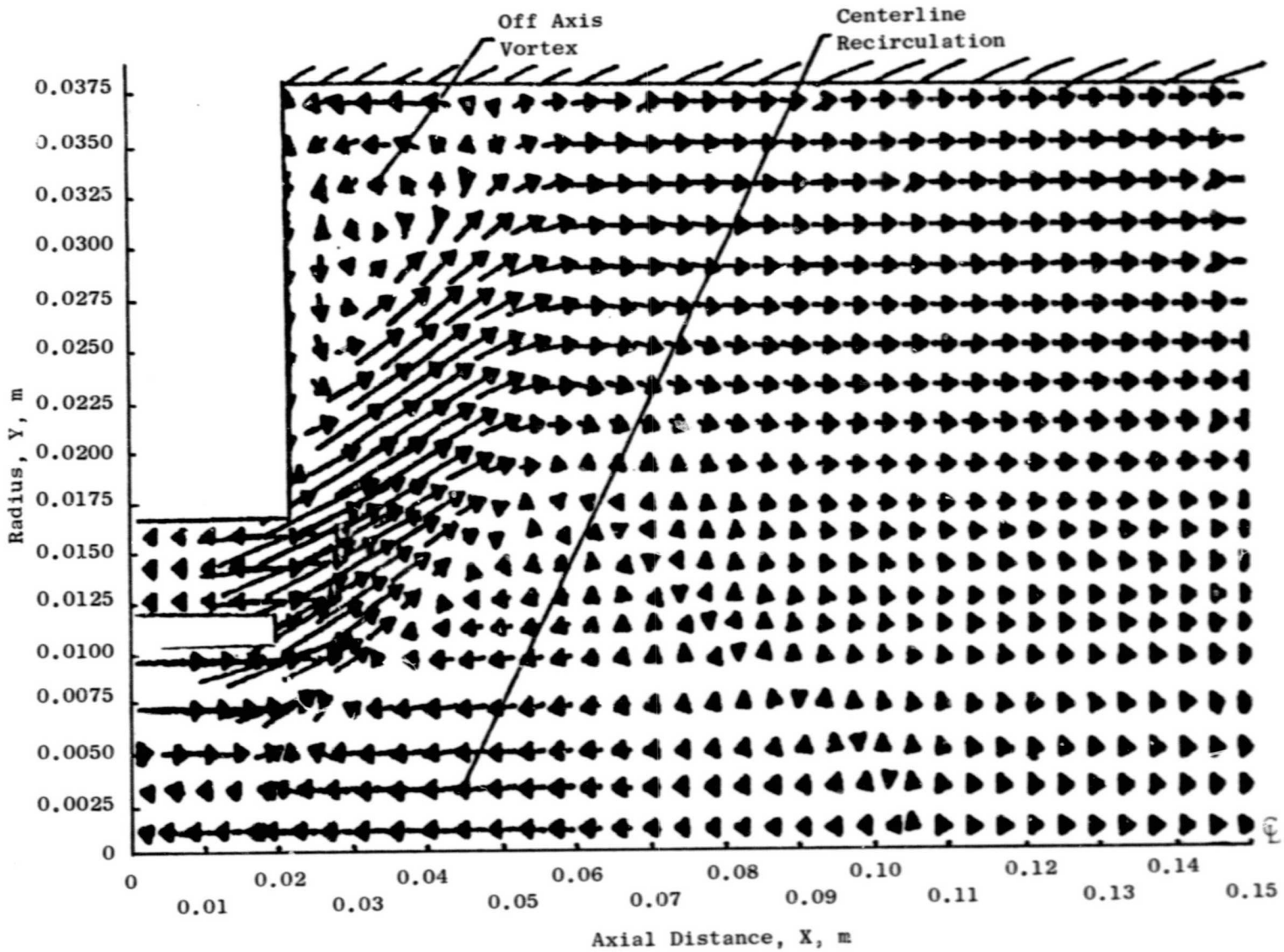

Figure 3. Velocity Field Calculation Using GETREF Code (2-D).

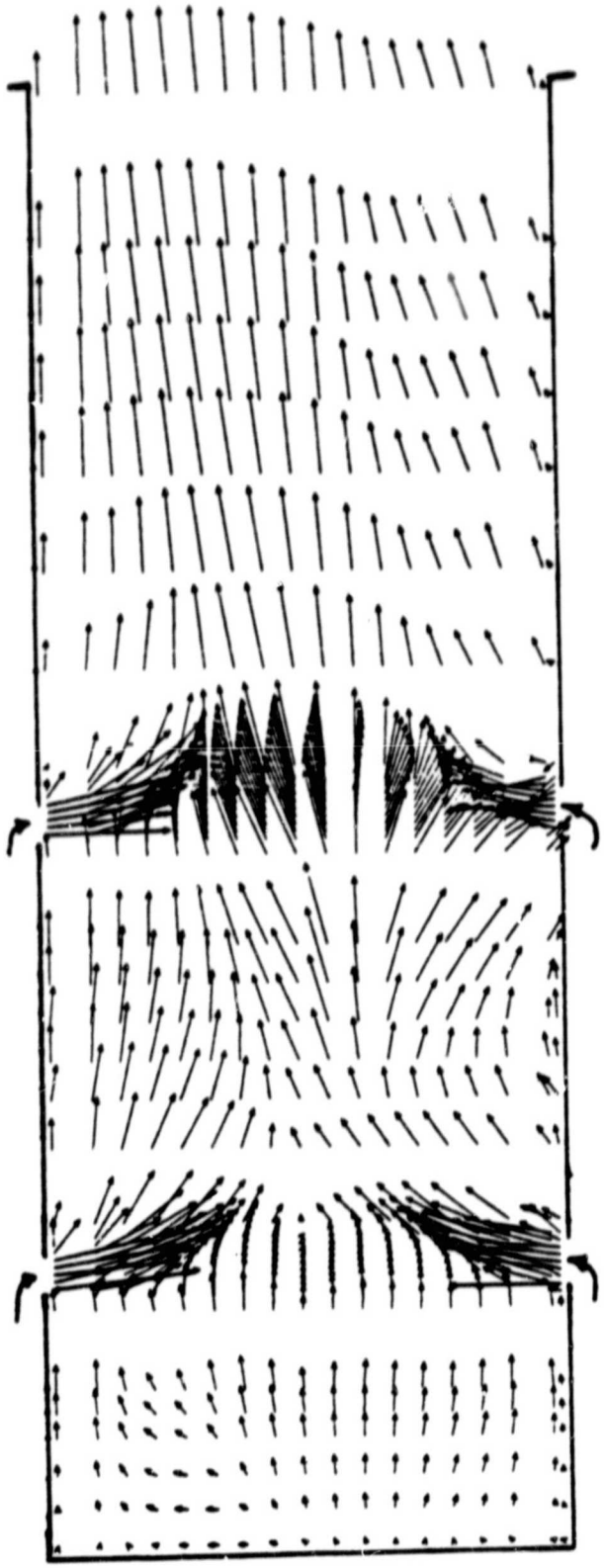

Figure 4. Calculated Velocity Field for a Combustor Using 3-D Elliptic Code (K Plane 15).

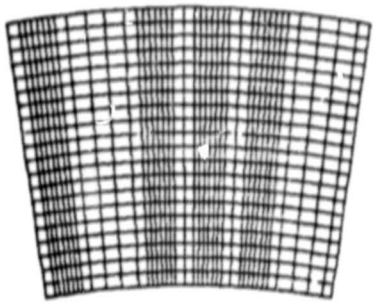

R-Theta Plane

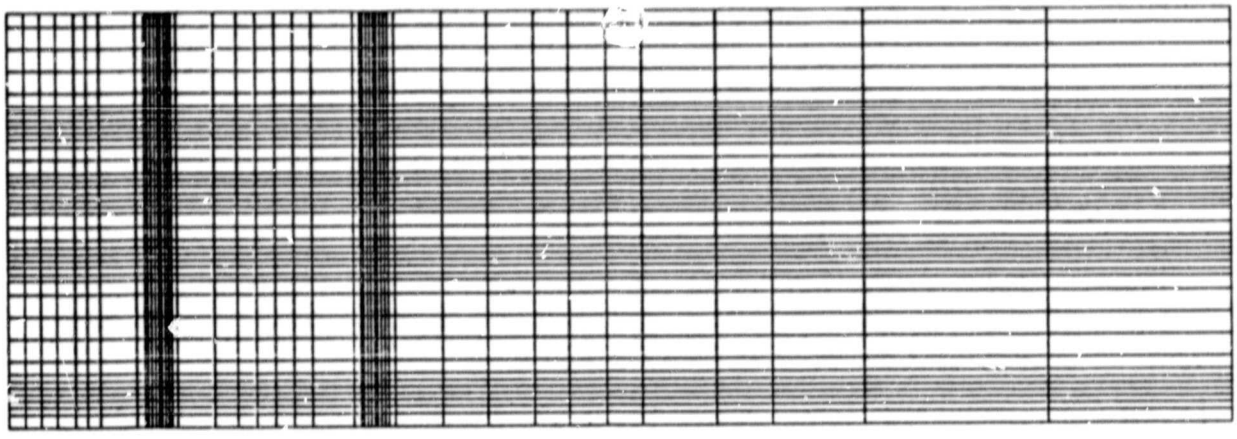

X-Theta Plane (Outer)

Figure 5. Grid Used in 3-D Calculation of Combustor (See Figure 4).

numerical diffusion. This produces mixing rates greater than specified by the turbulence model. Whenever the individual calculation cells have a Peclet number above 2.0, second order accurate central differencing numerics cannot be used and upwind differencing (first order accurate) is used which introduces significant numerical diffusion. Figure 6 shows that the cell Peclet numbers are below 2.0 in only isolated regions. Thus, without the ability to use much finer grids, the model inherently involves significant numerical diffusion for combustor flows. Claus, Reference 3, showed that, even when using a much more detailed grid for a single dilution hole than possible for a real combustor, analysis inaccuracy results from the numerical diffusion.

2. In order to introduce noncylindrical combustor walls the stairstep technique must be used and this involves grid concentration in unneeded regions and crudeness in calculating film cooled walls. In addition, with the rectangular grid system required with the 3-D codes, significant grid is wasted in regions external to the flowpath.

3. In the existing codes, the geometry-based swirl cup and fuel injection inputs do not correctly define the initial fuel distribution for all combustors. Swirl cups have been tested at General Electric with minor geometry changes that make major differences in metal hot streaks and exit gas temperature patterns; these geometry changes would not result in any change in the model input unless some knowledge (external to the computer program) of the nature of the flows emerging from the swirl cups was available.

Accordingly, improvements addressing these deficiencies must be evolved before the codes become the effective design and analysis tools suitable for designing combustors with enhanced durability.

- Shaded Regions Represent X Peclet Numbers Less Than 2

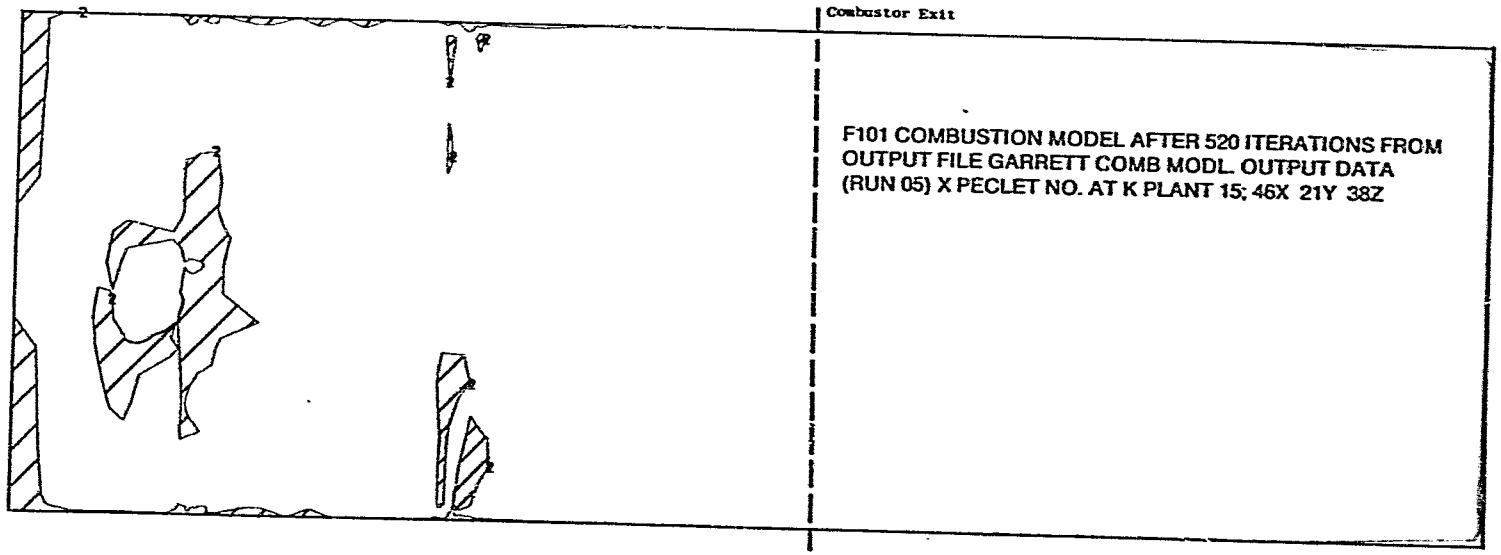

- X Peclet Number Contours in the Calculated Combustor Flow

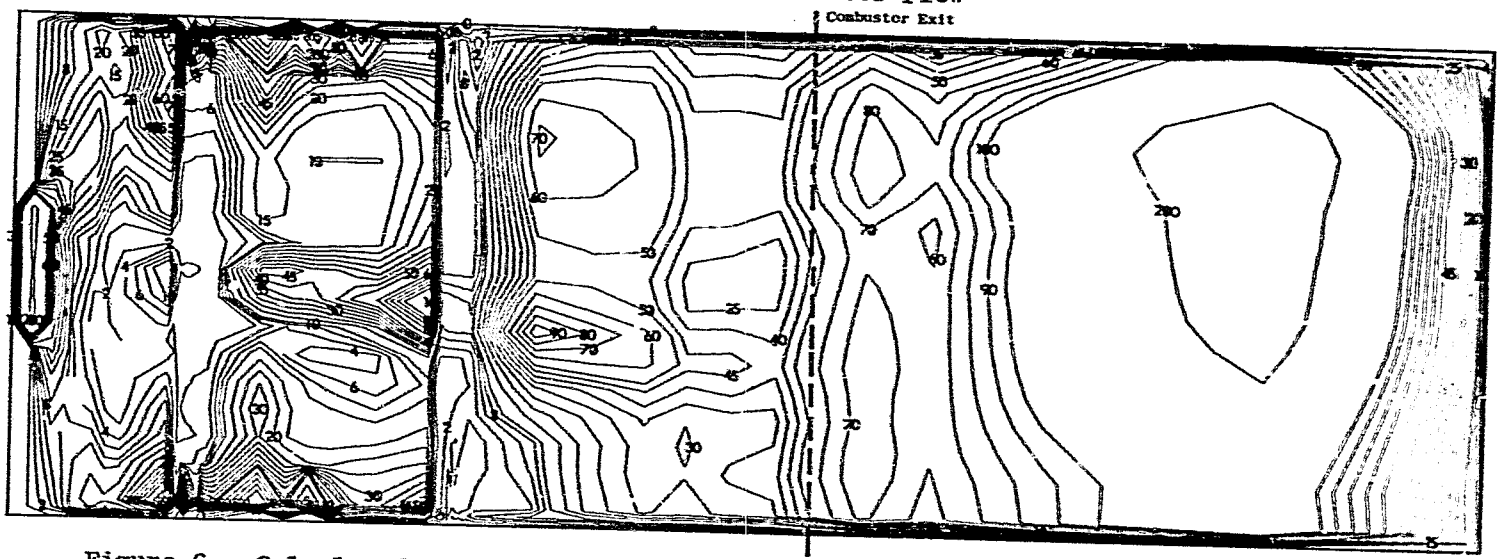

Figure 6. Calculated Peclet Number in the X-Direction from 3-D Combustor Calculation.

IV. PROGRAM APPROACH

The approach for assessing the modules already in general use at General Electric was accomplished by relatively straightforward comparisons with available General Electric data. The approach for assessing the Internal Flow Module was more complex and is discussed in the paragraphs below.

The assessment of the usability of the existing internal flow codes was conducted in two parts. The first part consisted of comparing "benchmark" quality data with the predictions from the axisymmetric elliptic research code (GETREF) and its parabolic version as applicable. These comparisons permit very methodical examinations of the mathematical techniques and the physical modules. Based on the results, general conclusions regarding future module development were then drawn.

The second aspect of the assessment addressed the usability of the 3-D code, INTFLOW. In these assessments, the methodical assessment of numerical error and the physical modules as conducted with the axisymmetric code GETREF was not attempted. The assessment approach was more the approach of the eventual engineer user rather than the original programmer. The objectives, therefore, included observation of the ease of input, convergence rate and computing time, and of the accuracy of the results. Primary focus was placed on the ability of the codes in two areas: (1) exit gas temperature prediction, and (2) hot gas side inputs to the Heat Transfer Module.

For exit gas temperatures, it was postulated at the outset that, even if the primary combustion zone (dome) flow fields were poorly predicted, a useful tool could still be developed if the dilution jet mixing process could be adequately calculated. An approximately correct dome flow analysis could be input and the subsequent dilution mixing calculation could be used to find the relative effect of some postulated dilution hole change.

In the case of the hot side inputs to the heat transfer calculation, again design usefulness could be expected with even somewhat limited accuracy of the internal flow calculation. First, the protection of the wall by the film cooling could still be dealt with by the present methods which involve the correlation of wind tunnel data for many film slots. Hence, only the hot gas side data just beyond the boundary of the film protection layer would be needed. It was recognized at the outset that the existing codes did not have a capability to predict flame radiation levels better than current estimating methods. The development of this capability and, hence, its evaluation was relagated to some future effort. Again, as in the case of the gas exit temperature patterns, an improved technique for inputting the air swirler and fuel flows into the dome would be needed to obtain this capability.

For real combustors, the basic flow field may be controlled much more by the pressure fields than by the turbulent shear layers prominent in simpler asymmetric experiments in the literature. For example, the length of a recirculation zone is a critical parameter in the axisymmetric experiments. In a

combustor, the recirculation zone length frequently ends just upstream of the first dilution hole location. Its length is predominantly controlled by the pressure field created by dilution holes rather than the turbulent mixing phenomena in the axisymmetric experiments. Thus, it may be possible to calculate reasonable combustor flowfields even though turbulent mixing is not being computed accurately; turbulence models with improved accuracy may not be essential. In the effort herein it was not presumed that combustor models needed to be as accurate or as detailed in all aspects as was needed for good comparisons with the simplified experiments. Thus, the efforts with the 3-D models were to see if useful results for durability design and development could be achieved, even though it was recognized that the node detail achievable with the storage limitations of the IBM 3081-D processor would be inadequate by the standards explored for the axisymmetric experiments.

The next section, Section V, describes the data selected to help assess the modules. This included data from General Electric combustors, data from simpler more difinitive experiments reported in the literature, and data from experiments conducted under this Aerothermal Modeling program. The experiments were structured to provide progressively increasing complexity from a simple dilution jet in a crossflow to a five combustor dilution pattern with and without combustion.

Section VI indicates the results of the assessment of the accuracy of the modules in current design use. Reasonable accuracy is demonstrated but the value of improved hot gas side inputs to the Heat Transfer Module is also recognized.

Section VII presents assessments by one and two dimensional studies. Numerics were studied analytically with specific examples while comparison of calculations with axisymmetric experiments was employed to further examine the mathematical and physical basis for combustor internal flow models.

Section VIII assesses the specific 3-D internal flow modules available in INTFLOW by comparison with 3-D experiments.

V. DATA SELECTED FOR COMPARISON WITH MODELS

Data for assessing the accuracy or deficiencies of the modules in this effort are available from three sources: (1) General Electric aircraft turbine engine combustor test data, (2) experiments in the literature, and (3) experiments conducted at General Electric in this program. The engine combustor data include the measured metal temperatures and exit gas temperatures, as well as measurements of the flows and pressures through the diffuser and the annular passages surrounding the combustor. While the temperature data may be sufficient for a check of the overall validity of the modules, these data alone do not provide sufficient detail to permit the individual sources of error within a given module to be identified, particularly the internal flow module.

On the other hand, geometrically simpler experiments which contain the same physical phenomena permit detailed probing of the flow field. Data obtained in such experiments are, therfore, defined as "benchmark" quality data for use in checking the mathematical/physical elements of the modules. Most of these experiments are two-dimensional for ease of data taking. This permits a more accurate assessment of the physics since, for example, numerical inaccuracies can be minimized by using more grid points per coordinate direction in the calculation plane.

Data from four axisymmetric "benchmark" experiments selected from available literature were chosen to assess the mathematical/physical modules. The first is an existing experiment performed at General Electric and consists of an axisymmetric-free fuel jet burning in a coflowing air (Reference 4). The primary reasons for its selection are (1) the removal of "numerical diffusion" errors since the governing equations become parabolic, and (2) the availability of high-quality Laser Doppler Velocimeter (LDV) and spontaneous Raman scattering data available. An unambiguous evaluation of the turbulence-chemistry interaction model could, therfore, be made. In addition to the jet experiment, three axisymmetric recirculating flow experiments were chosen: an isothermal annular dilution jet experiment (Reference 5), an isothermal double-swirled pipe flow (Reference 6), and a bluff-body stabilized non-premixed flame (Reference 7). These provide checks of the model under progressively more complex circumstances.

The above four experiments were analytically simulated using codes (elliptic GETREF or its parabolic version, as relevant) developed at General Electric.

For simple round dilution jet flows in a crossflow, a three-dimensional flowfield, data from the available literature (Walker and Kors, Reference 8) were chosen for examination. In the past, these data provided a large matrix of jet penetration data, permitting useful penetration correlations, Holdeman and Walker, Reference 9. These data and correlations have been used at General Electric in combustor design and development work.

To provide data from more complex flowfields, a series of experiments was devised and conducted as part of this Aerothermal Modeling Program. These experiments involved progressively more complex flows beginning with a row of jets in a crossflow, followed by opposing jets, alternate jets of different sizes, and a second row of dilution jets with the two row pattern simulating the dilution pattern of one General Electric combustor. The initial tests in this series were conducted with cylindrical inner and outer walls and a flat uniform inlet velocity condition. An illustration of the test rig used in these tests is shown in Figure 7. Tests with recirculation at the dome location and the two rows of dilution jets were introduced in two steps. First, a nonswirling dome flow with flow axisymmetrically diverging from the fuel nozzle position was tested, followed by a dome with counterrotating swirl cups like those used in a specific General Electric combustor. Then the true wall and dome contours of this combustor were introduced. All of the above tests were conducted without fuel injection. As in the Walker and Kors data, Reference 8, for the simple dilution jet, the approach flow was introduced at a different temperature than the dilution jets and detailed temperature measurements were the primary data. The experiments were then extended to include combustion, first with a gaseous fuel, that avoids considerations of fuel drop atomization and vaporization, and then with a liquid fuel. The effect of film slots was introduced in these last tests. A summary of each of the experimental test configurations is provided in Table I. The data was supplemented with nonburning data taken on the swirl cup and fuel nozzle assembly removed from the combustor.

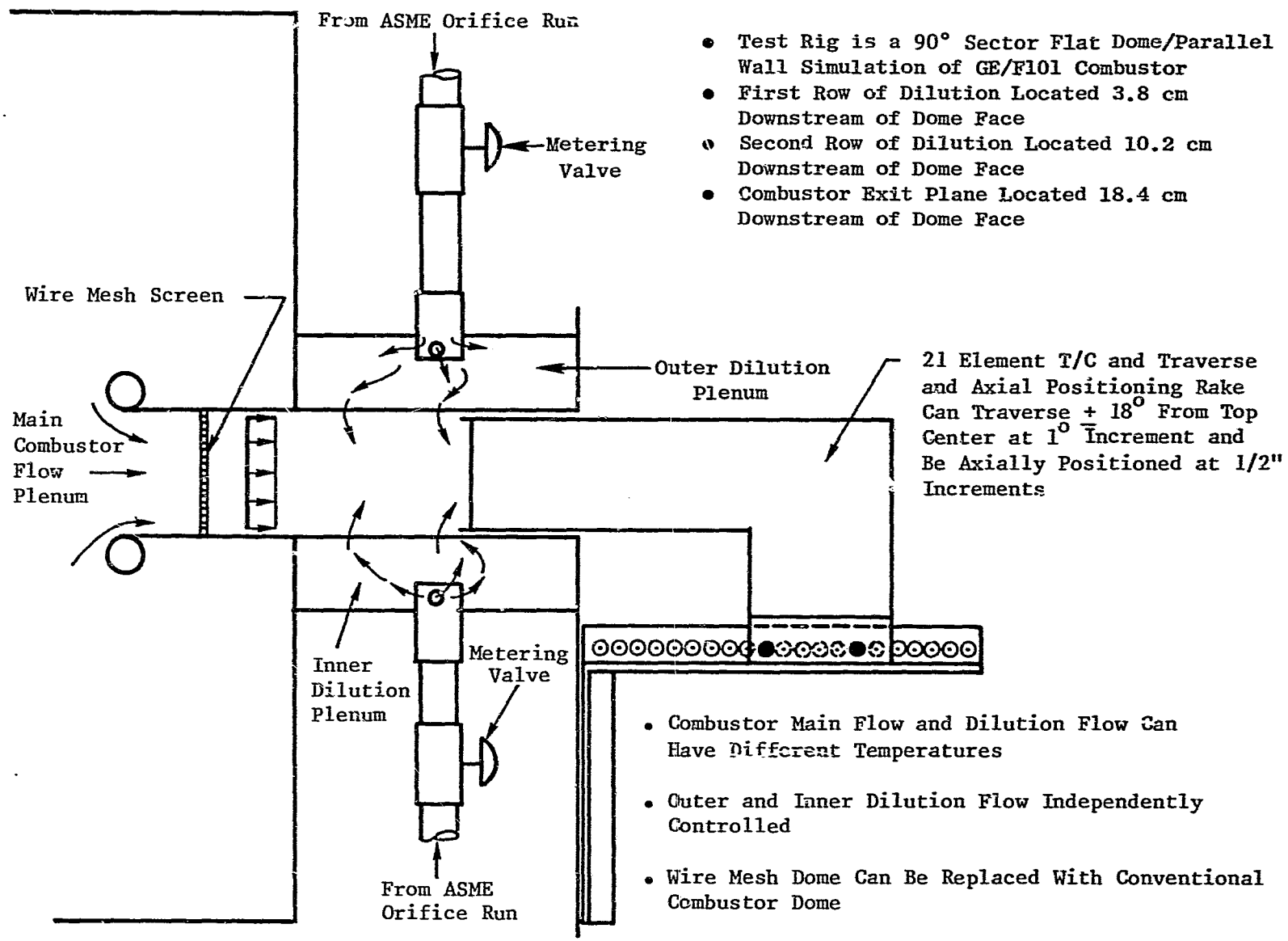

Figure 7. Aerothermal Modeling Experimental Test Rig (Unfueled).

Table I. Summary of Experimental Test Configurations.

Configuration	Outer Wall 1st Dilution Row	Inner Wall 1st Dilution Row	Outer Wall 2nd Dilution Row	Inner Wall 2nd Dilution Row	Dome Type	Wall Type	Fuel Type	Momentum Ratio
1	0.794 CM Diameter Spacing Every 9° From Top	None	None	None	Low AP Screen	Cylindrical - Bucoled	None	13
2		0.794 CM Diameter Spacing Every 9° From Top						12
3		None	0.794 CM Diameter Spacing Every 6° From 3° CM					15
4	0.794 CM Diameter 0°, 18°, 36° 1.032 CM Diameter 9°, 27°, 45°	0.794 CM Diameter 0°, 18°, 36° 1.032 CM Diameter 9°, 27°, 45°	None					10
5								50
6		0.794 CM Diameter 0°, 18°, 36° 1.032 CM Diameter 9°, 27°, 45°	0.913 CM Diameter Spacing Every 6° From 3° CM	0.913 CM Diameter Spacing Every 6° From 3° CM				10
7								
8		None	None	None				50
9		0.794 CM Diameter 0°, 18°, 36° 1.032 CM Diameter 9°, 27°, 45°	0.913 CM Diameter Spacing Every 6° From 3° CM	0.913 CM Diameter Spacing Every 6° From 3° CM	Perforated Plate 52 AP			50
10			None	None				50
11			0.913 CM Diameter Spacing Every 6° From 3° CM	0.913 CM Diameter Spacing Every 6° From 3° CM	Nonswirl Air Injectors			50
12			None	None	Counterrotating Swirl Cup			50
13			0.913 CM Diameter Spacing Every 6° From 3° CM	0.913 CM Diameter Spacing Every 6° From 3° CM				50
14					Nonswirl Air Injectors			770
15 (GE/F101 Sector)	Standard Configuration (Equivalent Areas) 0.794 CM Diameter 0°, 18°, 36° 1.032 CM Diameter 9°, 27°, 45°	Standard Configuration (Equivalent Areas) 0.794 CM Diameter 0°, 18°, 36° 1.032 CM Diameter 9°, 27°, 45°	Standard Configuration (Equivalent Areas) 0.93 CM Diameter Spacing Every 6° From 3° CM	Standard Configuration (Equivalent Areas) 0.93 CM Diameter Spacing Every 6° From 3° CM	Standard Configuration	Standard Configuration		Injection 52 M/Sec
16A (GE/F101 Sector)					Without Dome Cooling			Injection 44 M/Sec
16B (GE/F101 Sector)								Injection 29 M/Sec
17A (GE/F101 Sector)						Without Liner Cooling		Injection 44 M/Sec
17B (GE/F101 Sector)								Injection 29 M/Sec
17C (GE/F101 Sector)							JP-5 Low AP Injectors f/a = 0.016	Injection 160 M/Sec
17D (GE/F101 Sector)							JP-5 High AP Injectors f/a = 0.016	Injection 233 M/Sec
18A (GE/F101 Sector)					Standard Configuration	Standard Configuration	JP-5 Low AP Injectors f/a = 0.020	52 Pressure Drop
18B (GE/F101 Sector)							City Gas Low AP Injectors f/a = 0.012	52 Pressure Drop
18C (GE/F101 Sector)							JP-5 High AP Injectors f/a = 0.026	52 Pressure Drop
18D (GE/F101 Sector)							JP-5 High AP Injectors f/a = 0.012	52 Pressure Drop

VI. ASSESSMENT OF AEROTHERMAL MODELS CURRENTLY USED IN DESIGN/DEVELOPMENT

Calculations were made with the Diffuser Module, Flow Distribution Module, and Heat Transfer Module and compared with measured data from the General Electric F101 engine.

DIFFUSER MODULE

Comparison of the diffuser module calculation with measured results showed reasonable agreement. This calculation provides early in the design process a valuable estimate of the average pressure level in the three streams that feed the combustor, the dome region, outer annulus and inner annulus passages. However, early in the development process these pressures are measured in special diffuser rig tests. Diffuser development modifications are made early in the development process and frequently remain unchanged through subsequent combustor development efforts. Thus the basic inputs to the Flow Distribution Module during combustor development are available from measurements and the Diffuser Module is not a basic source of error. If, however, significant 3-D effects were present in these flows such as wakes from fuel nozzles or structural struts, they may not be adequately documented by the measurements or by the computer programs currently used. Three-dimensional analytical treatments could provide more detailed information than available from measurements. However, while some older combustor designs exhibited effects within the combustor and in the exit gas temperature patterns that were attributable to upstream wakes, for more modern General Electric combustor diffuser designs, there is no evidence of wakes affecting the flow through the combustor apertures. Thus, a refined 3-D treatment is not considered essential at this time to improve the accuracy of analysis for combustor durability. It is expected, however, that work on improved diffuser analysis methods including 3-D treatment will continue at General Electric.

FLOW DISTRIBUTION MODULE

Figure 8 shows comparisons of measurements with the calculations including specifically the overall check of pressure drop. There is some evidence of Reynolds number or approach turbulence levels affecting measured results because engine test results at high pressure with compressor discharge flow turbulence levels frequently show lower overall combustor pressure loss than one atmosphere combustor component test rigs. The flow coefficient correlations for individual apertures were derived generally from one atmosphere laboratory scale data. In general, the effects of two-dimensional passage flow including approach boundary layer flows have been adequately treated in the experiments that generated the flow coefficient data. Three-dimensional elliptic computer programs could be used/developed to calculate flow coefficients, flow angles, and flow distribution within individual aperatures and used as input to the Internal Flow Program.

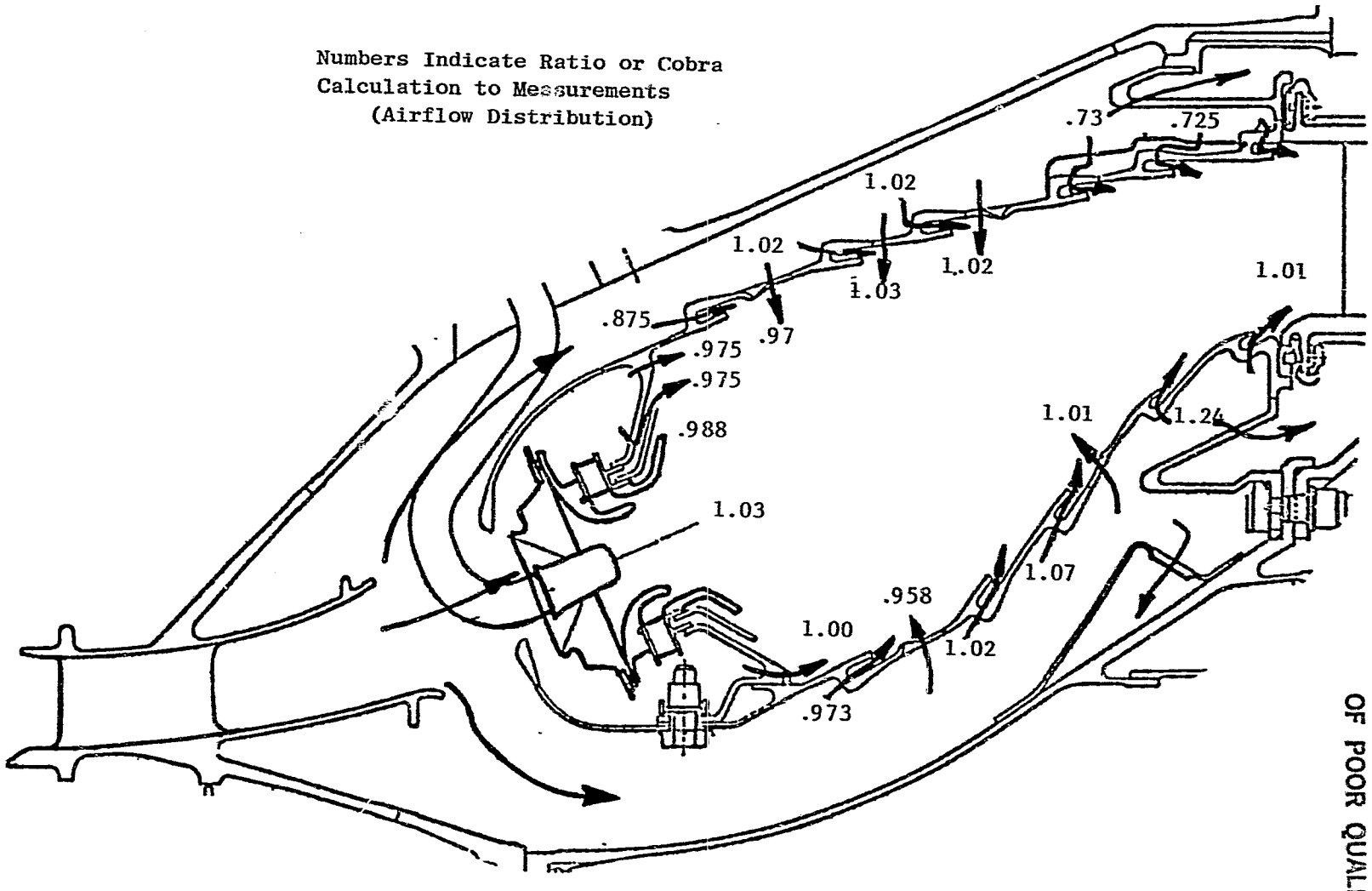

Figure 8. Ratio of Measured to Calculated Airflow Distribution.

However, the large collection oF flow coefficient and angle data and correlations for individual apertures available at General Electric allow accurate calculations without the aid of detailed flow analyses. Whenever new aperture shapes with unknown flow characteristics are introduced into designs or test hardware, additional laboratory tests of the individual aperture are routinely conducted for inputs into the Flow Distribution Module. This same flow information is also available for input into the Internal Flow Module. At this time, more accurate methods of determining flow coefficient and angle information for the Flow Distribution Module are not significantly limiting the accuracy of General Electric's overall Aerothermal Module.

HEAT TRANSFER MODULE

Figure 9 compares calculations of the Heat Transfer Module with measured metal temperature data along a General Electric combustor liner. The agreement is reasonable as should be expected from the nature of the module. Within the module, heat transfer conduction within the metal structure is calculated by routines that have been long in use at General Electric with well established accuracy. The convective heat transfer calculations are based on well established correlations in general use as modified by data and specific flow features that might be expected to alter the correlations. Wind tunnel data on special local heat transfer coefficients are measured and correlated where appropriate and introduced into the Heat Transfer Module calculation method. Film slots introduce cooling air along the hot side of the combustor wall which helps protect the surface from the hot combustor gases. Wind tunnel data on the effectiveness of cooling air to protect the surface are available at General Electric from a large variety of cooling slot designs, and for substantially new slot designs new wind tunnel data is obtained. These data/correlations are utilized in the Heat Transfer Module. The hot gas side inputs of velocity, temperature, and flame radiation are estimated from previous experience guided by forcing the heat transfer calculations to agree with metal temperature measurements. The selection of these input values is the greatest source of error in the Heat Transfer Module. It is planned that the Internal Flow Module will in the future be able to supply more accurate values and a more detailed distribution of values than is available at present. The accuracy would be improved if hot gas side velocities and temperatures were available from a sophisticated Internal Flow Module even if the radiation still had to be estimated from calculations beginning with measured metal temperatures. It is expected that this temperature and velocity capability will become available well before reliable flame radiation calculations are available from the same three-dimensional calculated internal flow field.

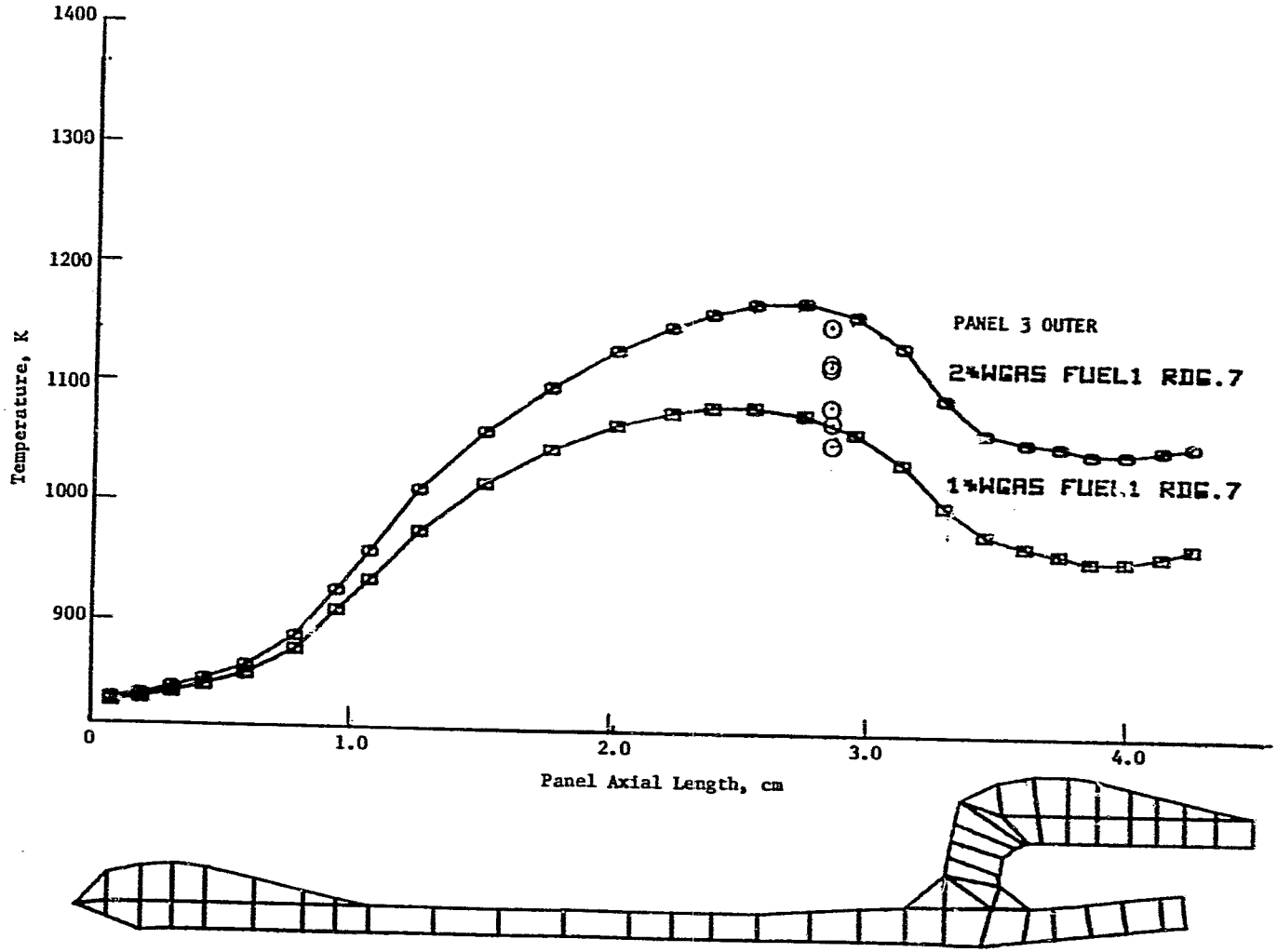

Figure 9. Comparison of Measured to Calculated Liner Metal Temperatures.

VII. ASSESSMENT OF MATHEMATICAL AND PHYSICAL BASIS OF INTERNAL FLOW MODULES BY ONE- AND TWO-DIMENSIONAL STUDIES

The aerothermal model of the combustor internal flowfield - distinguished from a particular code - can be regarded as a set of simultaneous partial differential and algebraic equations, a discretization procedure and a solution algorithm. Physical modeling is contained in the original equations, mathematical accuracy in the discretization procedure and solution algorithm, and speed of convergence primarily in the solution algorithm. It is computationally prohibitive and even unnecessary to study these issues in 3-D flows although that is the eventual application. Thus, a series of one- and two-dimensional studies was conducted ranging from analysis of linear uniform coefficient convection-diffusion equations to a turbulent recirculating, combusting flow. These studies each focus on different aspects of the overall mathematical/physical model to assess their role in the accuracy of the eventual code.

The first issue studied was the accuracy of finite-difference representations of the convection term. Several finite difference schemes for approximating this first-order spatial derivative in convection-dominated flow were studied. The relative accuracy and efficiency (convergence speed) among the first-order upwind scheme, first order skew-upwind scheme, second-order central differencing scheme, second-order upwind scheme, and the QUICK scheme were compared against several idealized one- or two-dimensional model problems, e.g., uniform, constant diffusivity flow with a prescribed source term.

It was shown that in a finite difference simulation with large-cell Peclet number, the high wave number Fourier components of the real solutions cannot be evaluated accurately. As a result of this, in a convection-dominated flow, if the viscous terms are required to balance the convection terms in a thin layer close to the downstream boundary due to, for example, a Dirichlet-type boundary condition being applied there, a finite difference approximation can, at best, use the truncation errors of the approximations to help damp out the disturbances in that thin layer. The detailed structure of the real solution is unresolved. Even this may or may not be accomplished by a given scheme, and hence for a high cell Peclet number flow the formal order of accuracy, by itself, is a poor criterion by which to judge the performances of different schemes. For example, Figure 10 compares the typical solution profiles along the y-direction given by the five schemes for a 2-D convection-diffusion equation with constant values of u, v, and Pe (Pe = 40, u/v = 2). In Figure 10, the downstream boundary conditions are taken to be the same as the upstream boundary conditions. Figure 11 shows the solution profiles given by the five schemes for the same flow problem but with zero as the downstream boundary condition; a thin boundary layer normal to the flow direction is formed close to the downstream boundary. Among the five schemes tested in this study, the second order upwind scheme gives the most satisfactory results in general; this scheme, however, still exhibits some overshoots in the solution. On the other hand, although both second order central differencing and QUICK are formally of the same order of accuracy as the second order upwind scheme, they

$$u\phi_x + v\phi_y = 0,\ 0 \le x \le ,\ 0 \le y \le 1$$

$$\phi(0, y) = 100y^n ,\ 0 \le y \le 1$$

$$\phi(x, 0) = 100\left(\frac{x}{\cot\theta}\right)^n ,\ 0 \le x \le 1$$

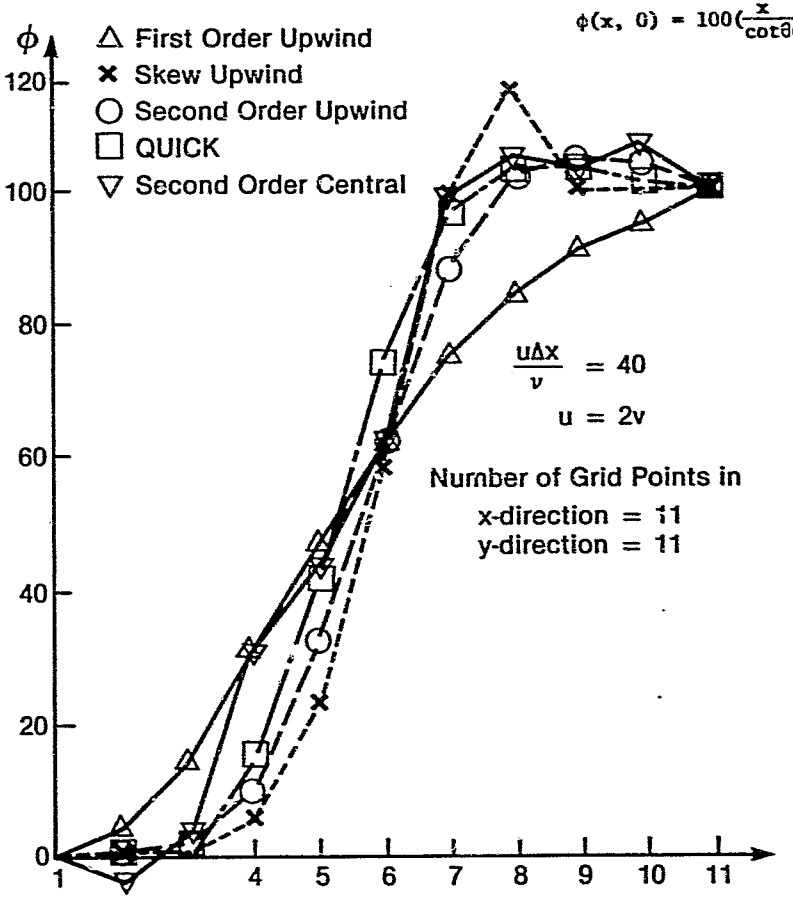

Figure 10. Numerical Solutions at x = 1 - 2Δx (Downstream Boundary Conditions: Gradient of φ = 0 in Streamwise Direction).

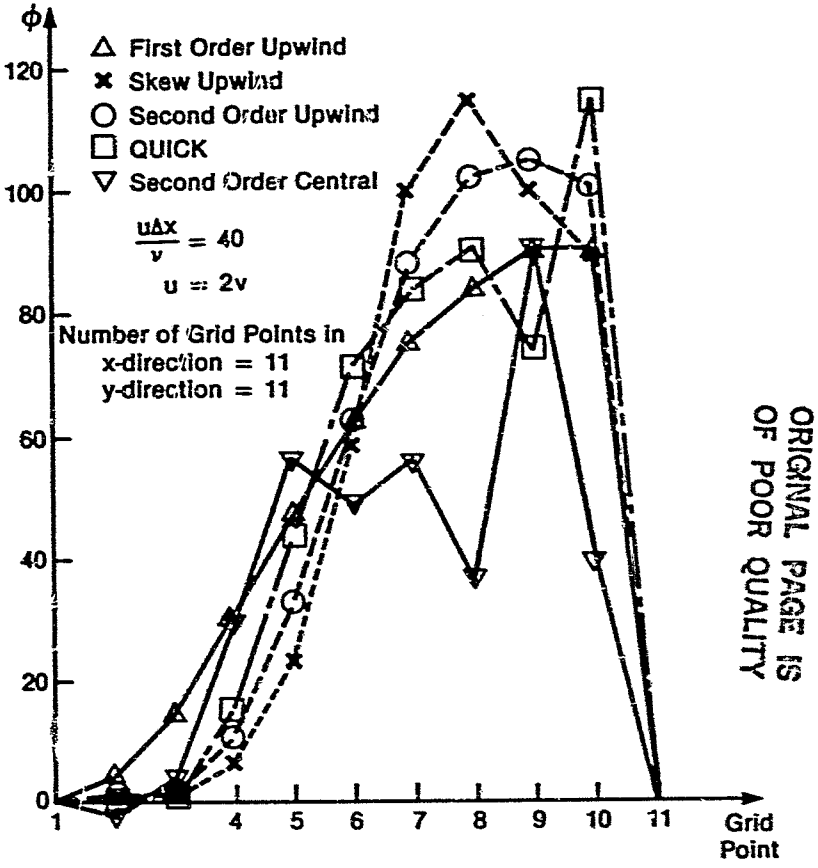

Figure 11. Numerical Soulutions at x = 1 - 2Δx (Downstream Boundary Conditions: φ = G).

fail to enhance the viscous terms properly where needed for a high cell Peclet number flow problem. Noticeable spurious oscillations appear in the numerical solutions. It should be noted that the magnitude of spurious oscillations in the solution by QUICK are generally less serious than those by second order central differencing. Furthermore, if no boundary layer type region exists in the real solution, the accuracy of the approximating solutions given by QUICK and that by the second order upwind are comparable. The first order upwind scheme is free from unphysical over- and undershoots in the solutions for all the test problems considered, but fails to give accurate approximations in the presence of a source term and shows too much numerical diffusion in the convection-dominated region for multidimensional flow. The skew upwind scheme is able to substantially reduce numerical diffusion by the first order in the cross stream direction but is found to be less satisfactory than the second order upwind scheme. The skew upwind scheme also fails to give accurate solutions in the presence of source terms. For all the formally second order accurate schemes studied here, the standard over-relaxation technique could not be applied for large values of cell Peclet number; a modified relaxation factor yielded convergent solutions for all cases considered.

The physical models for turbulence and turbulence-chemistry interaction phenomena were studied by comparison of predictions with four "benchmark" quality axisymmetric experiments. These experiments were: a turbulent non-premixed jet flame, an annular isothermal dilution jet/chamber flow; a co- and counterswirler isothermal pipe flow; and a non-premixed, bluff-body stabilized flame. The turbulent jet flame is a shear flow and so a parabolic version of the model was used. The elliptic code GETREF was used for the three recirculating flow simulations.

The first simulation establishes the need to account for random compositional and temperature fluctuations and validates the recommended probabilistic model. In a shear flow such as this jet flame the parabolic nature of the governing equations makes the issue of discretization accuracy irrelevant. Thus, a more direct assessment of the turbulence and particularly the turbulence-chemistry interaction model is possible. In additon, the jet flame experiment provided both laser velocimeter and spontaneous Raman scattering data so that the mean, variance, and, indeed, the pdf (probability density function) of major species concentrations, temperature, and axial velocity were available. Comparisons of these quantities many of which are shown in Figures 12 through 17 indicate the accuracy of the single-scalar pdf/equilibrium chemistry submodel in accounting for the highly nonlinear "unmixedness" turbulence-chemistry interaction. It should be noted that so-called adequacy of simpler models such as the eddy breakup scheme is often inferred from far more complicated experiments, e.g., recirculating flows with less precise instrumentation; under these circumstances the turbulence-chemistry interaction cannot be isolated and compensating errors frequently occur. Finally, it should be noted that the single-scalar pdf can be extended to multiscalar pdf descriptions of nonequilibrium flows without added empiricism.

The three recirculating flows are progressively more complex in that more phenomena occur simultaneously. Solutions essentially free from "numerical diffusion" were obtained by increasing grid density until central differencing

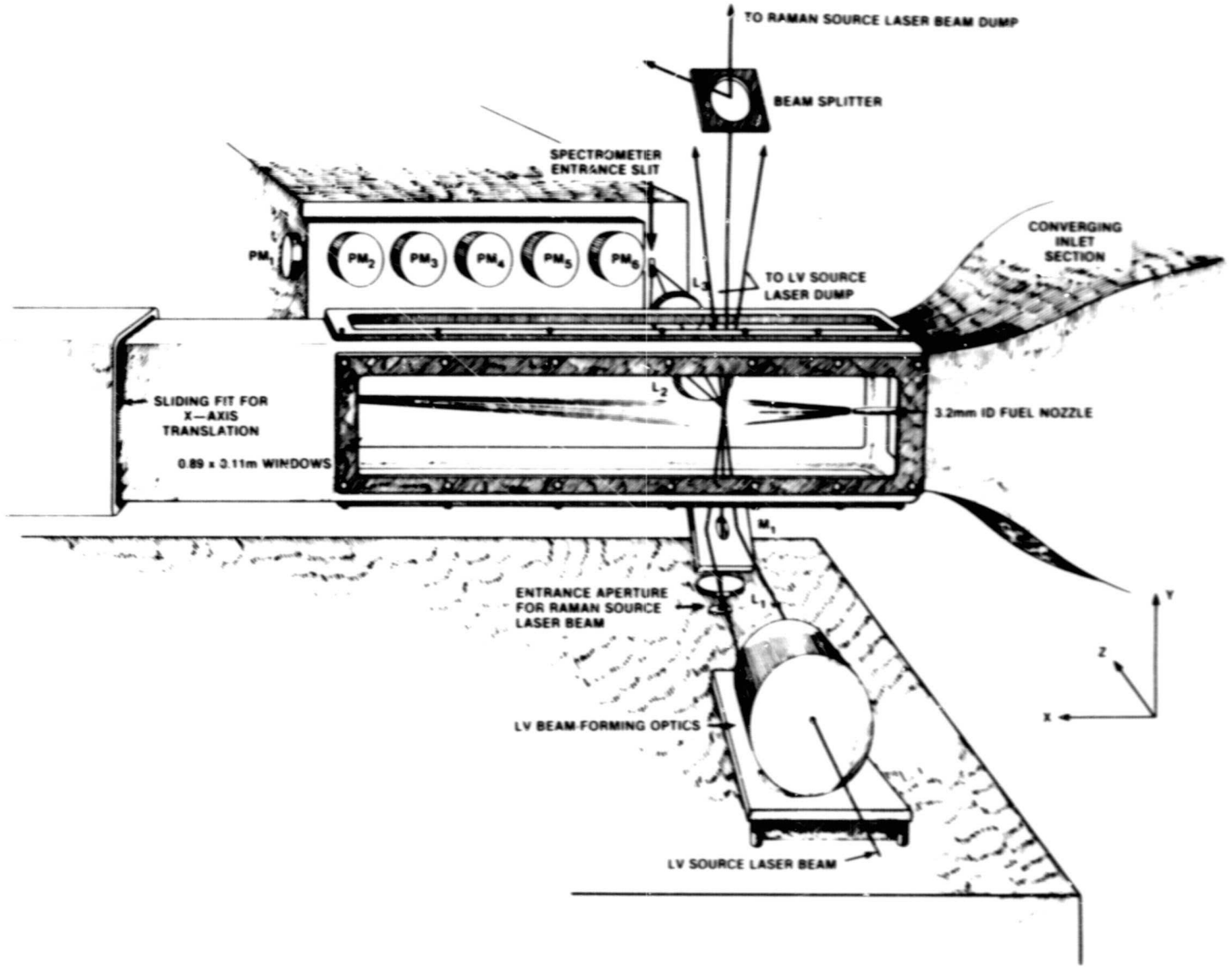

Figure 12. Burning Turbulent Diffusion Jet with LDV and Pulsed Raman Data.

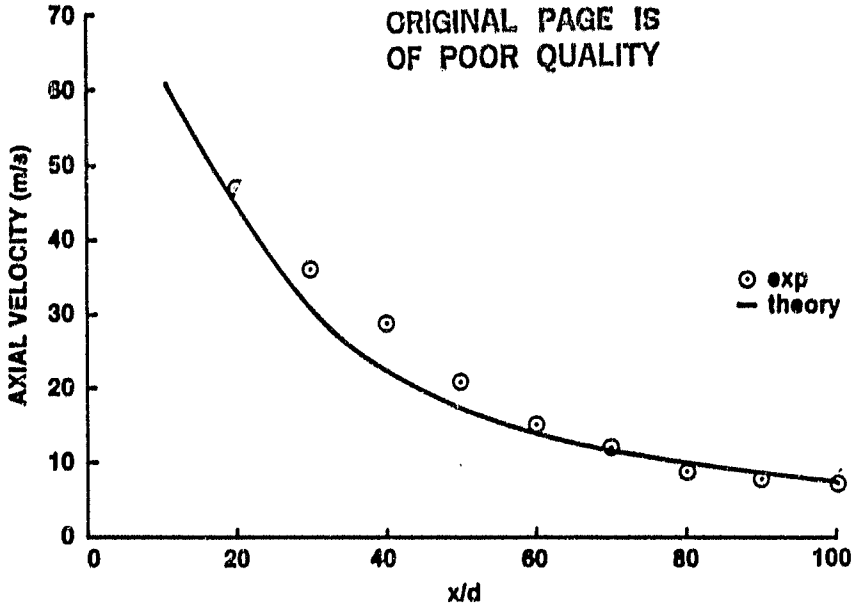

Figure 13. Centerline Profile of Axial Velocity.

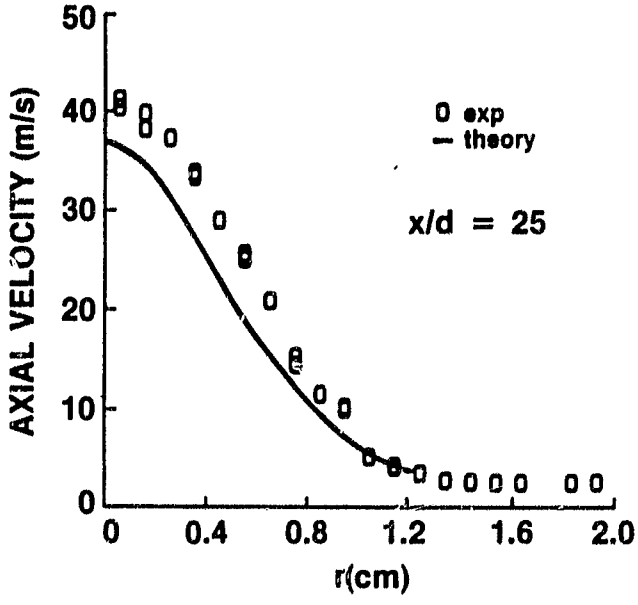

Figure 14. Radial Profile at Axial Velocity.

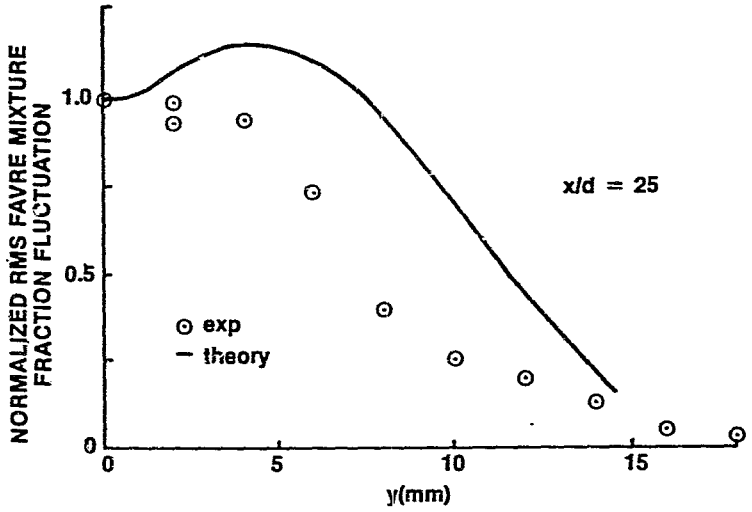

Figure 15. Radial Profile of Favre-Averaged Varianace in Mixture Fraction.

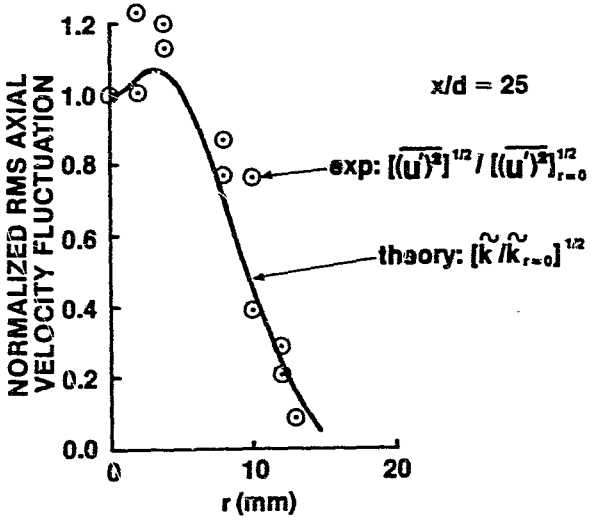

Figure 16. Radial Profile of Turbulence Kinetic Energy.

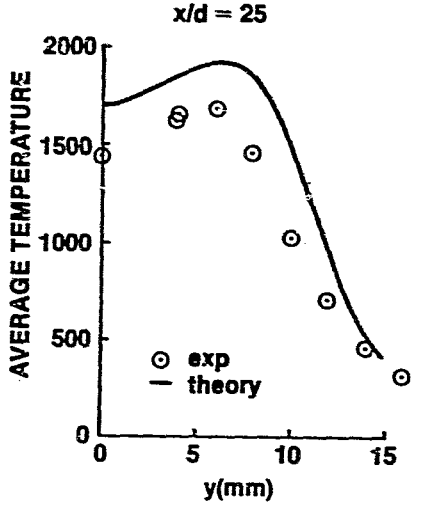

Figure 17. Radial Profile of Favre-Averaged Mean Temperature.

of the convection term was possible. The isothermal dilution jet/chamber flow provides data for a gas-turbine combustion chamber-like flow which retains axisymmetric geometry. Comparisons (Figures 18 and 19) indicate that the flow is dominated by the mean pressure-gradient rather than by the turbulence. This is evident from the poor agreement in the turbulence kinetic energy profiles and - despite this - the good agreement in the mean axial velocity However, in a reacting flow the turbulence is important in that besides controlling diffusivity, it interacts nonlinearly with the chemistry to produce a mean density field which enters all the equations.

The co- and counterswirled isothermal pipe flow (Figure 20) features strong streamline curvature and consequently, anisotropic turbulence. This cannot be represented by the isotropic eddy viscosity two-equation models which are widely used, e.g., k-ε model. On the other hand the full Reynolds stress equations - which could account for anisotropy - involve semiempirical closure for higher correlations, ignore very important issues in the dissipation rate equation, and are computationally very much more expensive. Hence, an algebraic simplification of the Reynolds stress equations which finally retains the two- equation form though with a very complex eddy viscosity, rather than a constant, was derived. This model is more universal than for example, Richardson Number corrections; it has been used successfully in several recirculating flows. Figures 21 and 22 show centerline axial velocity profiles in this flow with the standard k-ε and the new model; the appearance of a recirculation zone in the latter case confirms its accuracy.

The last flow simulated was an axisymmetric recirculating non-premixed flame (Figure 23). Combustion, i.e., the turbulence-chemistry interaction, was represesnted by the single-scalar pdf described earlier. Again, truncation error analysis and grid densification were used to produce solutions essentially free from numerical diffusion error. The centerline mean axial velocity profile (Figure 24) shows reasonable agreement with the data. The measured turbulence kinetic energy profile (Figure 25) shows a marked peak at the first stagnation point, which is not predicted. Mean and variance of species concentrations were not measured and so those predictions could not be evaluated. Agreement on mean temperature (Figure 26) is reasonable but it should be noted that in the model temperature is not a primitive variable, that thermocouple data is notoriously difficult to interpret, and that intermittency may affect the pdf in the annular shear layer (y = 0.07 m). The position of the forward stagnation point as a function of the central jet- to-annular flow velocity ratio (Figure 27) also shows reasonable agreement with the data.

The one and two-dimensional axisymmetric studies addressed the issues of stability and accuracy of convection term discretization, the performance of several difference operators in various flows, and the physical modeling of turbulence and turbulence-chemistry interactions. These studies all lead to modeling approaches which would result in a more accurate predictive capability in the next generation code for combustor flow.

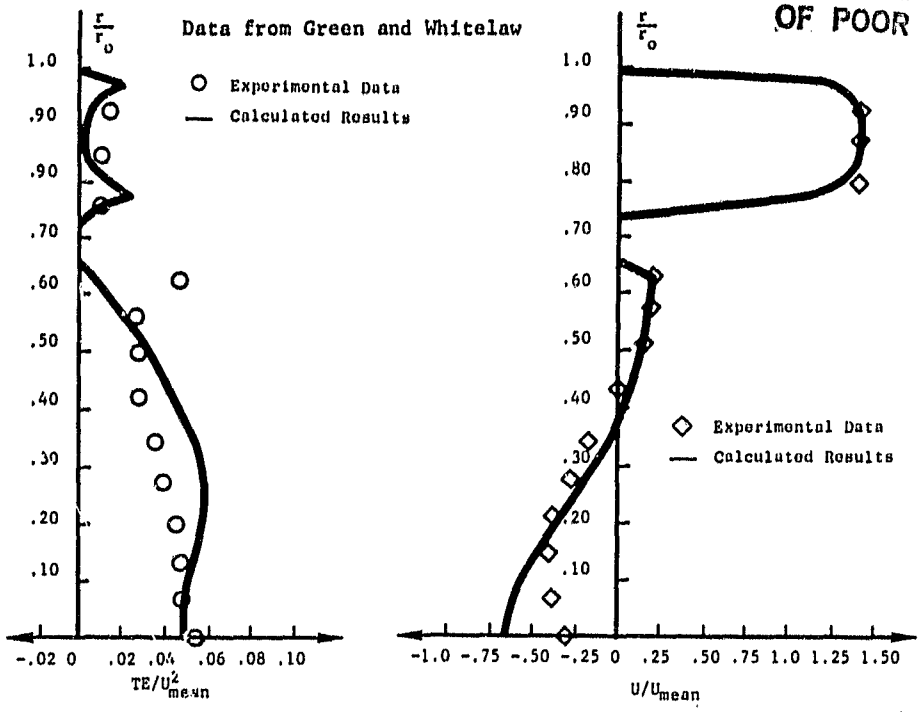

Figure 18. Radial Profile of Turbulence Kinetic Energy and Mean Axial Velocity at $x/r_o = -0.61$.

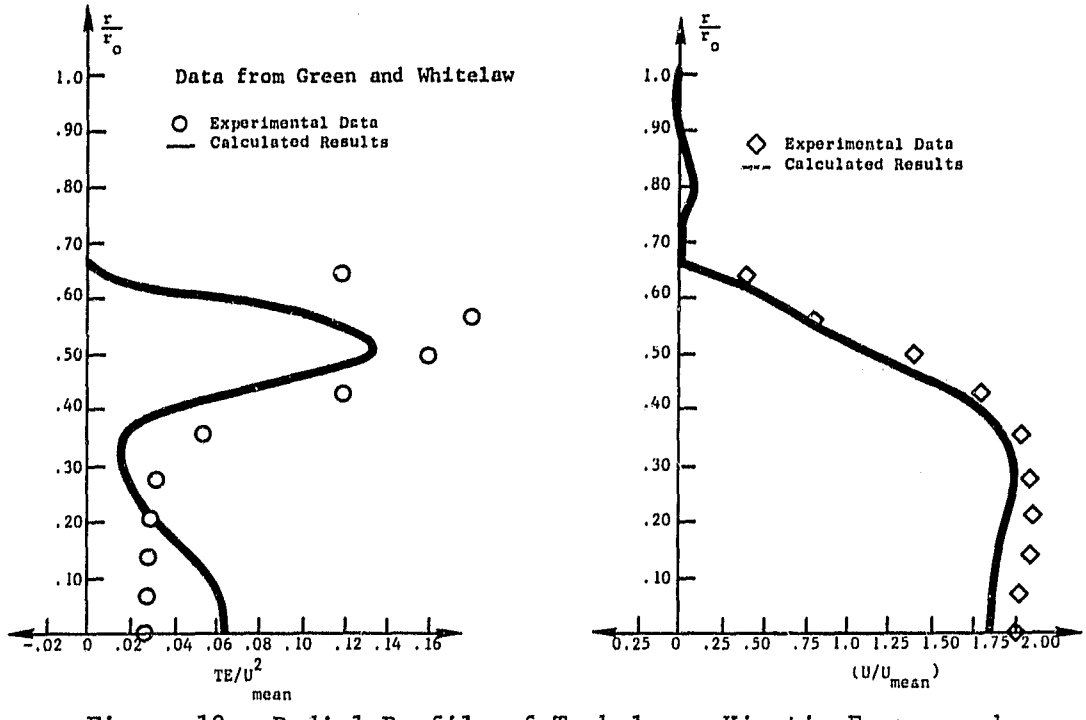

Figure 19. Radial Profile of Turbulence Kinetic Energy and Mean Axial Velocity at $x/r_o = 2.77$

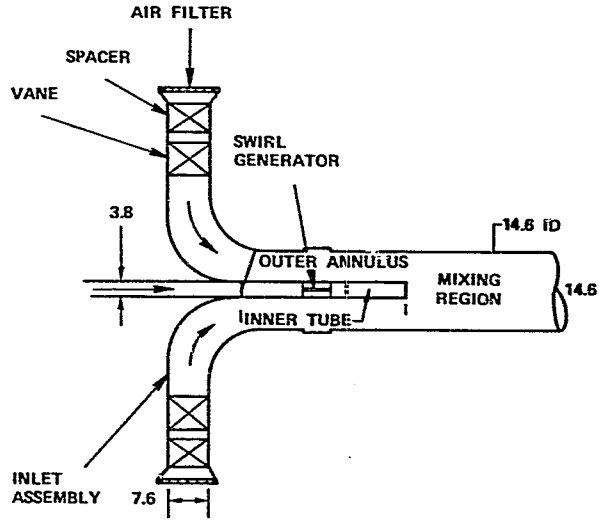

Figure 20. Experimental Flow Assembly Schematic.

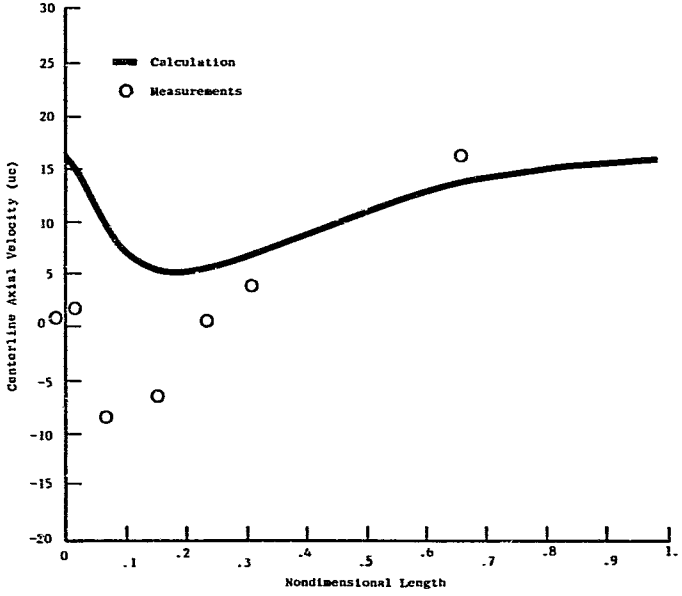

Figure 21. Centerline Profile of Axial Velocity for Counterswirl Flow, k-ε Model.

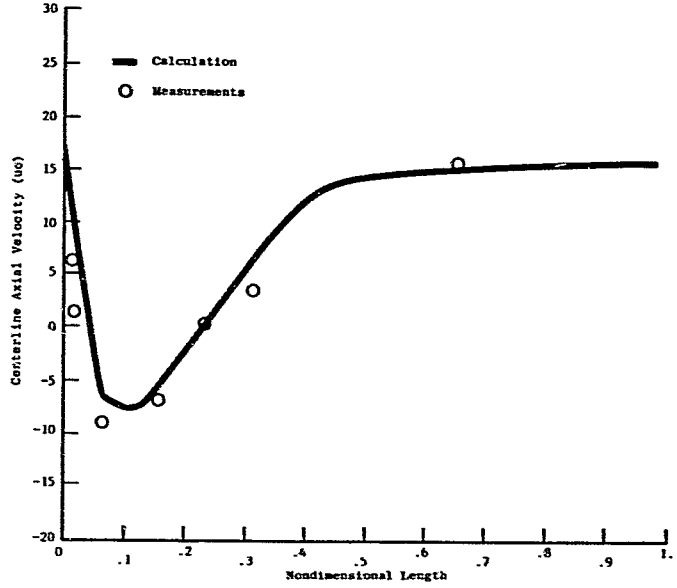

Figure 22. Centerline Profile of Axial Velocity for Counterswirl Flow, Algebraic Stress Model.

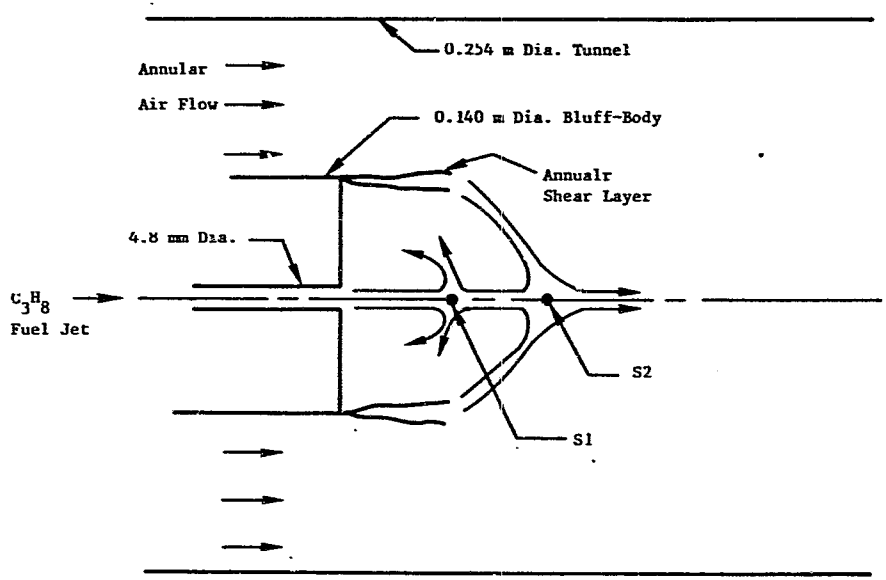

Figure 23. Schematic of AFAPL Axisymmetric Bluff Body Flame Experiment.

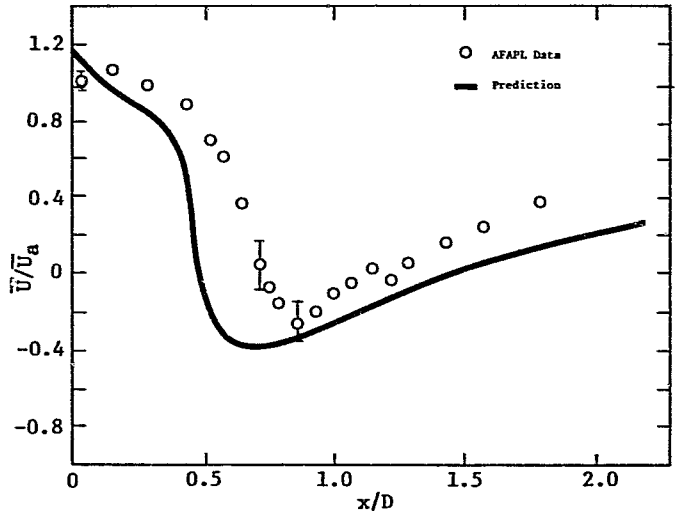

Figure 24. Centerline Axial Velocity

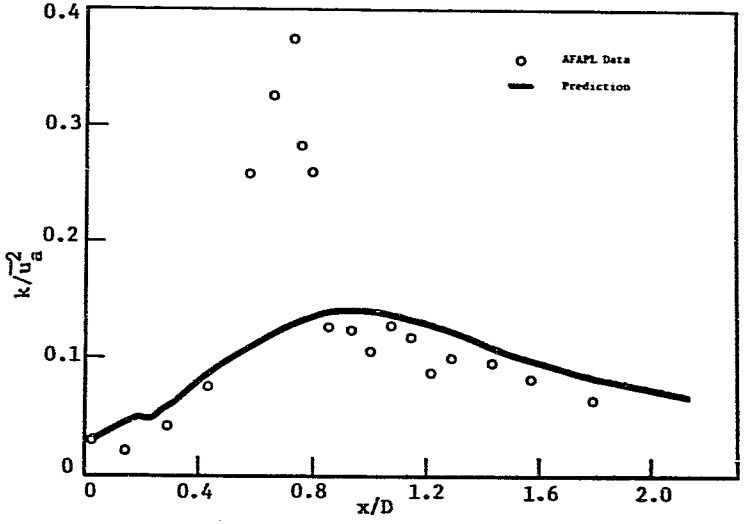

Figure 25. Centerline Turbulence Kinetic Energy.

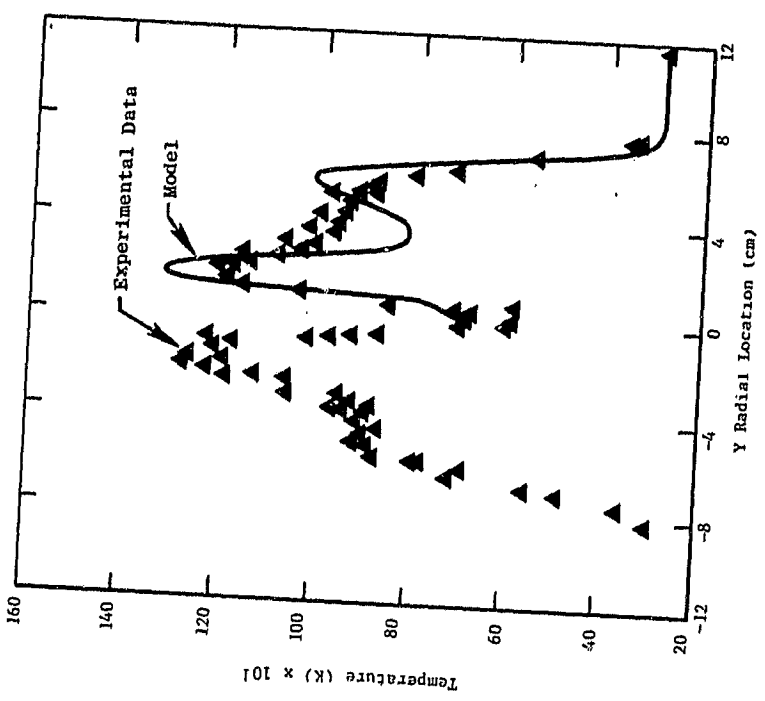

Figure 26. Radial Temperature Profile at X/D = 0.43.

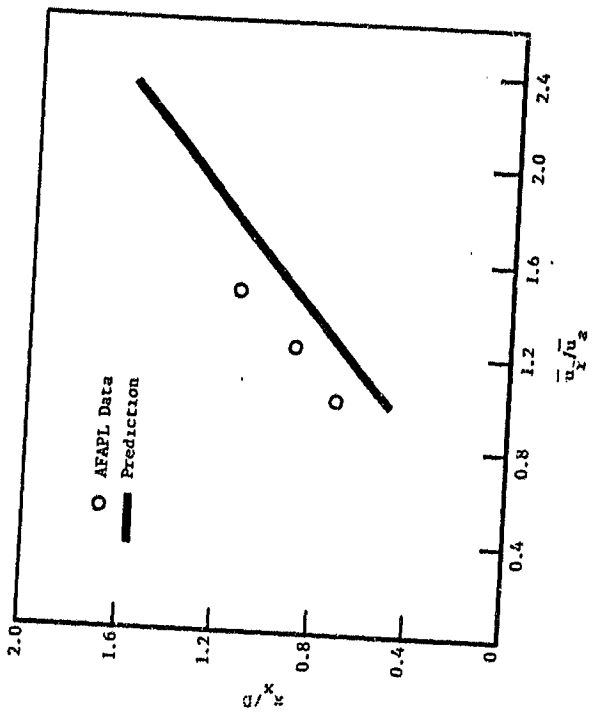

Figure 27. Location of First Stagnation Point for Higher Jet Velocities.

VIII. ASSESSMENT OF 3-D INTFLOW MODULE

The initial assessment studies were conducted using the Northern Research and Engineering Company, 3-D code, and data from Experiment 67 of the Walker and Kors experiments (Reference 8). In the first of this series of studies, an evaluation of three different grids was conducted, a coarse grid of 10395 nodes, a medium grid of 21000 nodes, and a detailed grid of 41600 nodes. The detailed grid, shown in Figure 28, requires nearly all the storage capacity currently available in the IBM 3081D computer system at General Electric. Figure 29 shows a comparison of the calculated jet penetration with the Holdeman and Walker correlation (Reference 9) of the Walker and Kors data. A comparison between the calculated temperature distribution obtained with each of these grids, and the measured test data at a distance of four hole diameters downstream of the injection point is presented in Figure 30. The calculated results after sufficient iterations generally agree with the jet penetration observed from the measured test data. The more detailed grid required a greater number of interations. The calculated temperature levels, however, differ considerably from the measured test data.

The next study conducted with this data involved examining the impact of the approach flow turbulence input parameters to see if greater mixing could be generated resulting in calculated temperature levels closer to the measured test data. From this study, it was determined that the length scale parameter had the greatest impact on the calculated turbulence levels and the jet temperature dissipation rate. Figure 31 presents a comparison of calculated results using the detailed grid (41600 nodes) along with an optimized set of turbulence input parameters, with the measured test data at a distance of four hole diameters downstream of the injection point. These results are considerably better than those observed in Figure 30.

This same set of turbulence input parameters was next applied to calculations of the higher momentum ratio Experiment 69 from the Walker and Kors experiments. Using the medium grid of 21000 nodes, gross over penetration was calculated. Only by using a significantly larger jet turbulence length scale was the calculated penetration reduced sufficiently to provide a close match with the measured test data.

The exact same calculation, as above, was also performed using the 3-D code assembled by the Garrett Turbine Corporation. A comparison between the calculated results obtained from the Northern Research 3-D code, the Garrett Turbine 3-D code, and the measured test data is presented in Figure 32. It is observed from these results that the two codes produce very similar and accurate results in terms of jet penetration and temperature levels. However, as observed in Figure 33, the calculated turbulence levels within the flow field differ considerably between the two codes.

Additional calculations of the lower momentum ratio Walker and Kors Experiment 67 test case were performed using the exact same turbulence inputs

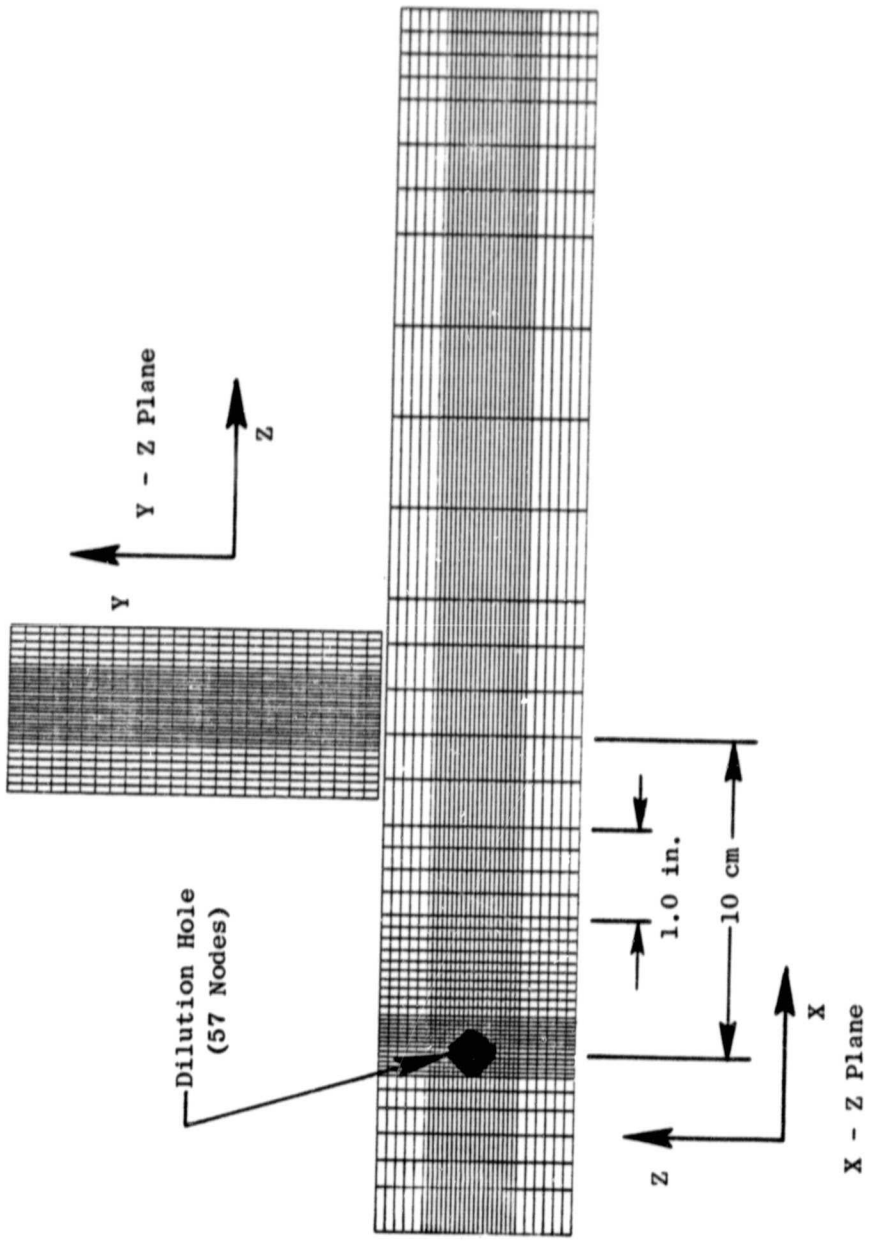

Figure 28. Grid 3 (Detailed) 50X 26Y 32Z.

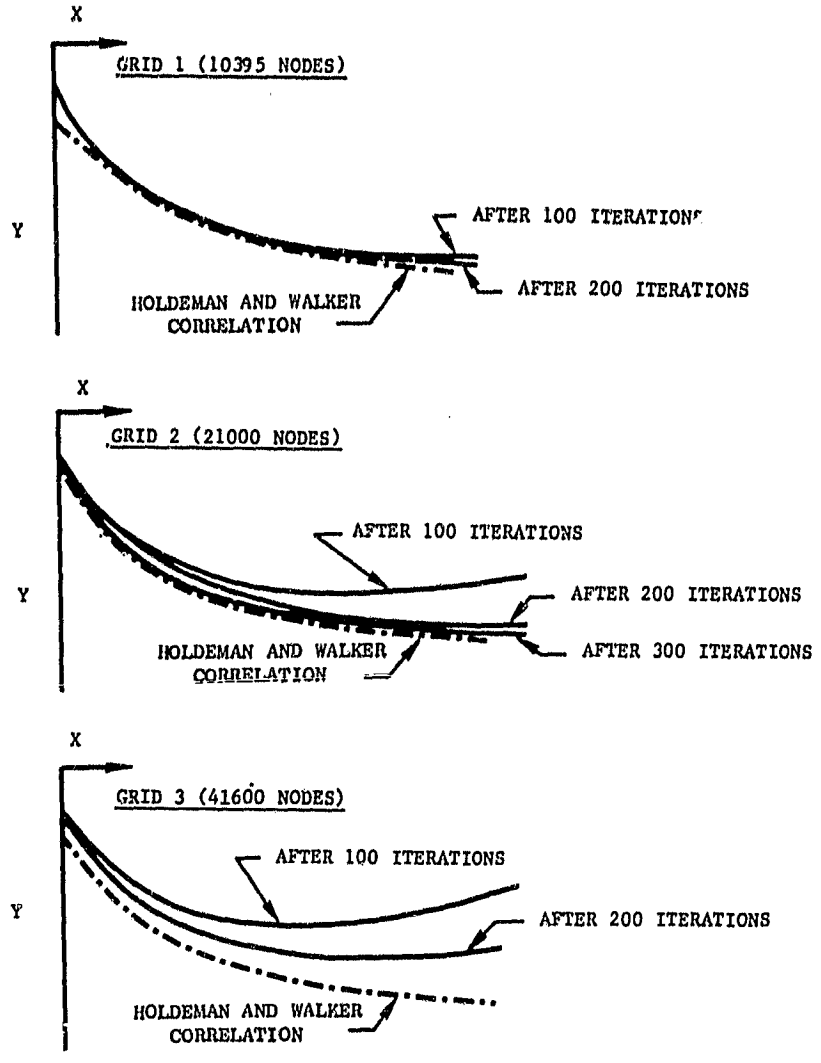

Figure 29. Comparison of Calculated Jet Penetration with Holdeman Correlation for Walker and Kors Exp. 67.

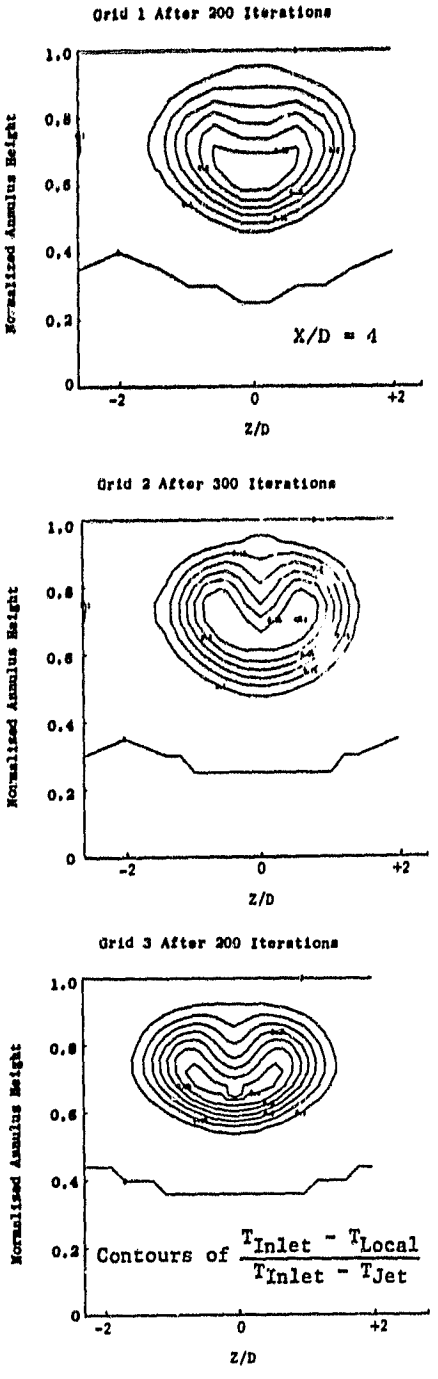

Figure 30. Calculated Results of Walker and Kors Exp. 69 Using Coarse, Medium, and Detailed Grids.

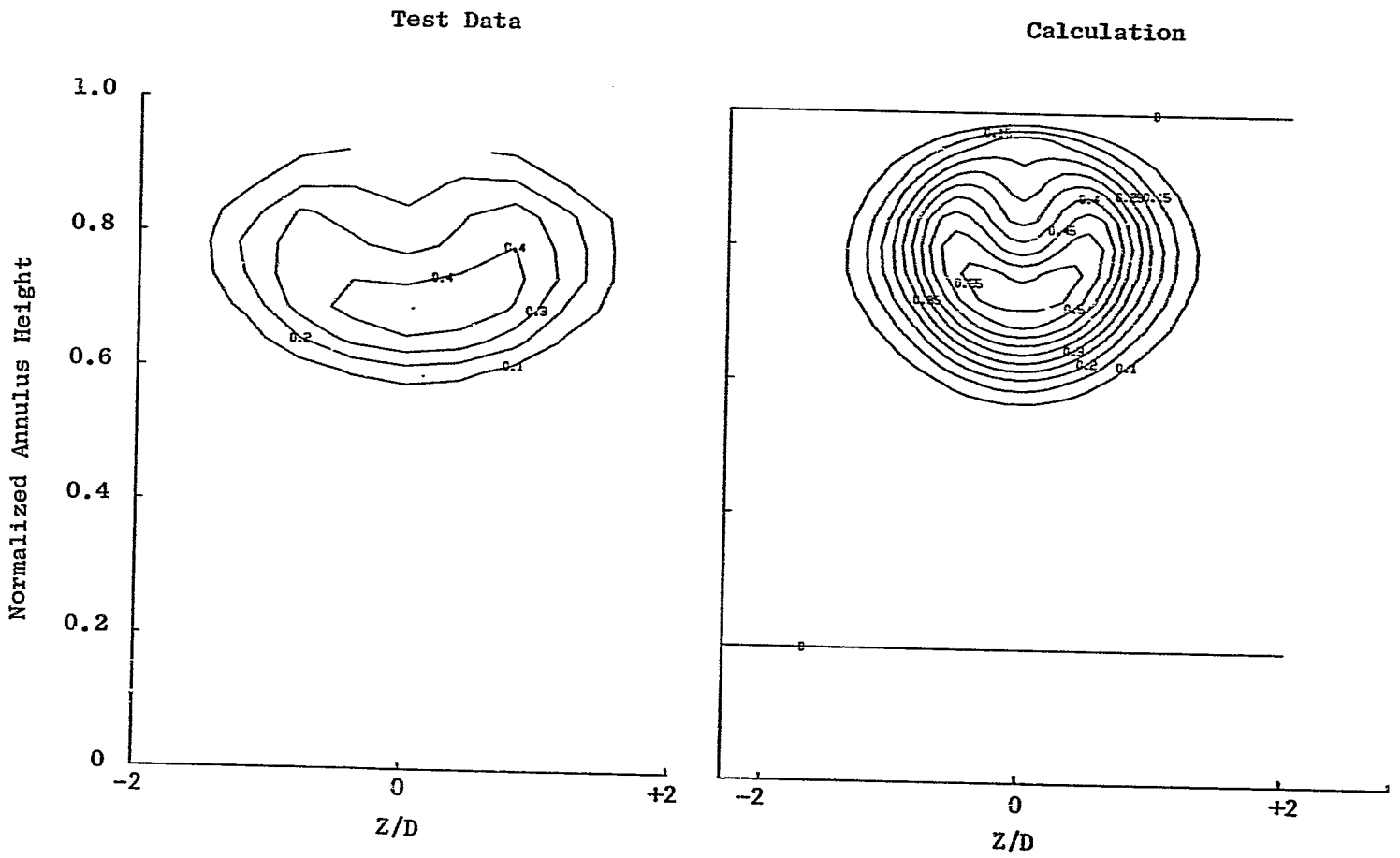

Figure 31. Calculated Results of Walker and Kors Experiment 67 Using Detailed Grid and Optimized Turbulence Inputs, X/D = 4.

Contours of $\frac{T_{Inlet} - T_{Local}}{T_{Inlet} - T_{Jet}}$

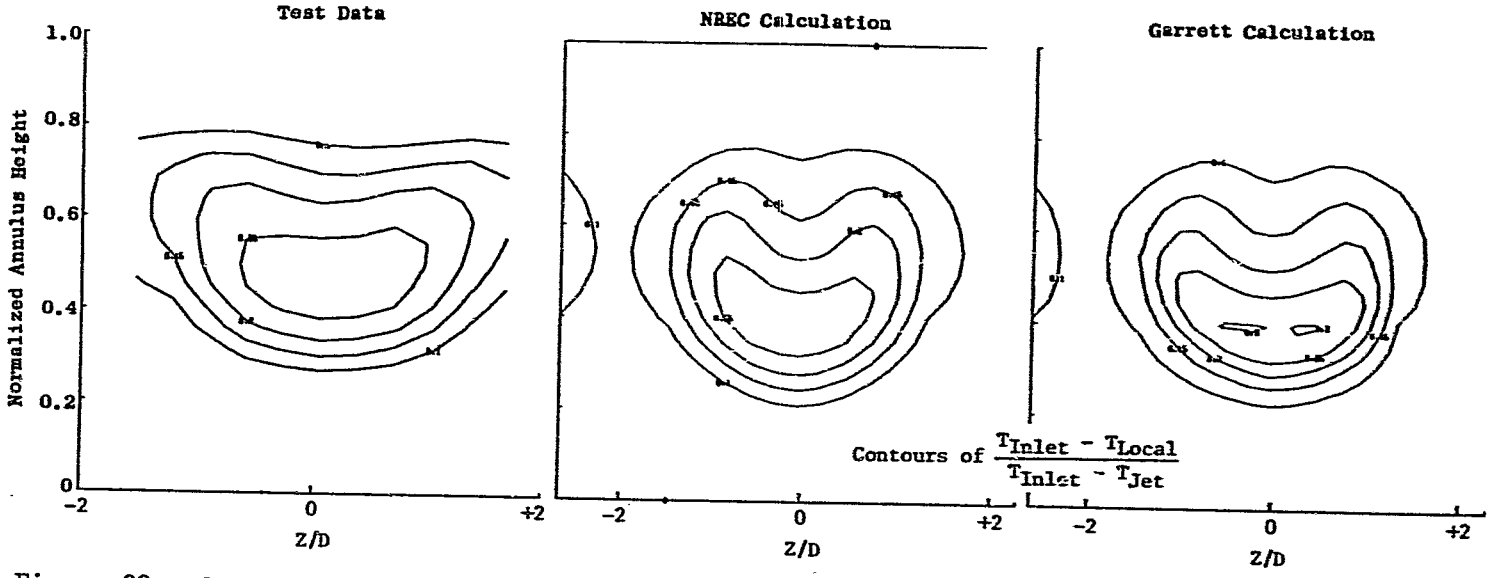

Figure 32. Comparison of Calculated Results of Walker and Kors Experiment 69 Obtained from the Northern Research and Garrett Codes, X/D = 4.

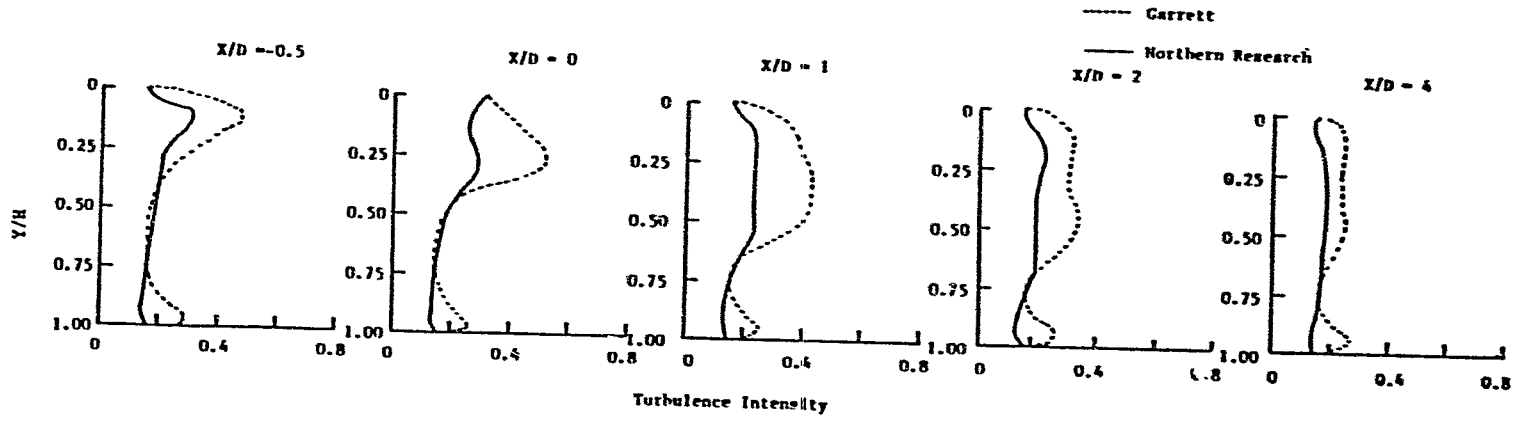

Figure 33. Comparisons of Calculated Results of Walker and Kors Experiment 69 Obtained from the Northern Research and Garrett Codes.

that provided the best agreement with the higher momentum ratio jets. These results showed some under penetration when compared to the measured test data, see Figure 34. One would expect the turbulence input parameters which produced satisfactory results in the calculations of the Walker and Kors Experiment 69 test case to also produce satisfactory results for the Experiment 67 test case. This observed problem is awkward in that a user of these codes must have beforehand knowledge of the turbulence inputs to use to produce accurate results.

Additional assessments of the 3-D internal flow code were performed by modeling selected experimental configurations tested as part of the Phase I effort. The test configurations selected represented progressively more complex internal flow fields. One of these configurations involved fuel injection with heat release. A coarse grid was selected to use in most of these calculations because of the excessive run times and costs associated with more detailed grids. This coarse grid, shown in Figure 35, contained 13365 total nodes. A detailed grid was selected to use in modeling the experimental configuration featuring fuel injection and heat release. This detailed grid, shown in Figure 36, contained 36708 total nodes. The calculations of these modeled experimental configurations used the same turbulence inputs that had produced satisfactory results in the calculations of the Walker and Kors Experiment 69 test case. This seemed appropriate because the experimental test configurations modeled featured dilution jets of high momentum ratio. The results obtained from these calculations are compared to the measured test data in Figures 37 through 43. The calculated results of the experimental test configurations without fuel using the coarse grid show over penetration of dilution jets and slower mixing rates (see Figures 38-43). However, in the case of the experimental configurations with fuel injection and heat release using the more detailed grid, the calculation accurately predicted the location of the hot spots (regions of high pattern factor) in the exit gas flow field (see Figure 43). This result is perhaps fortuitous since the model assumptions made concerning fuel injection and parallel wall boundaries represent gross approximations to the actual test case. Measured swirler discharge velocities were used for input to the 3-D model. In spite of the agreement of calculated results with the general character of the flow, the results demonstrated were not accurate enough to be directly useful in defining the development features of design pertabations needed for combustor durability analysis purposes.

The calculation of the experimental test configuration with fuel injection and heat release using the detailed grid, (Figure 43), was run for 800 iterations at a cost exceeding $7000. Despite this excessive run time, the solution is still not completely converged. As shown in Figure 6, the grid detail used in this calculation is not sufficient to provide all Peclet numbers below 2.0 throughout the calculation domain, thus numerical diffuser errors are introduced. Introduction of sufficient grid to achieve all Peclet numbers below 2.0 and, hence, accurate central difference numerics throughout the calculation domain is not practical with the current 3-D codes. A modest increase in grid by a factor of 3 in each direction would result in an overall factor of 27 in storage requirement, with significant increases in computational costs. Improved numerics that avoid the numerical diffusion error

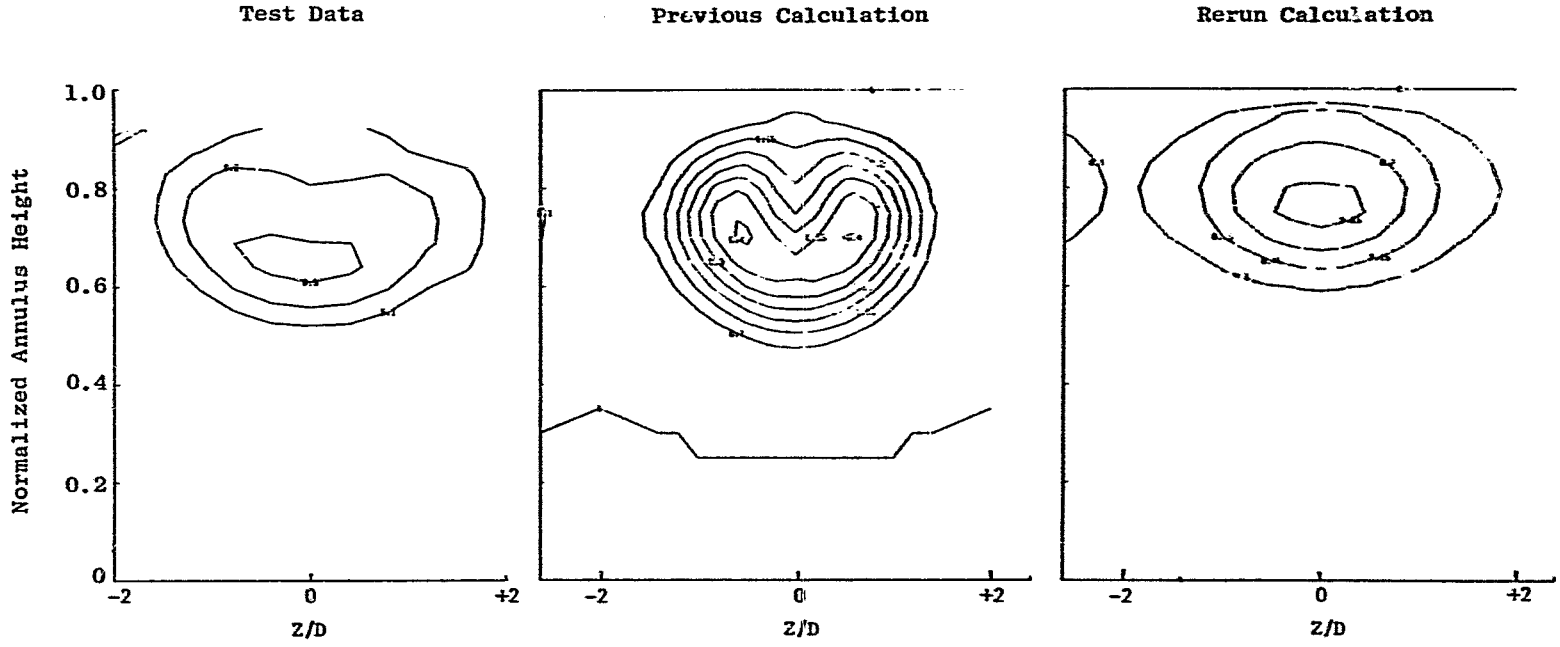

Figure 34. Calculated Results of Walker and Kors Experiment 67 Using Medium Grid with Larger Jet Turbulence Length Scale, X/D = 4.

Contours of $\frac{T_{Inlet} - T_{Local}}{T_{Inlet} - T_{Jet}}$

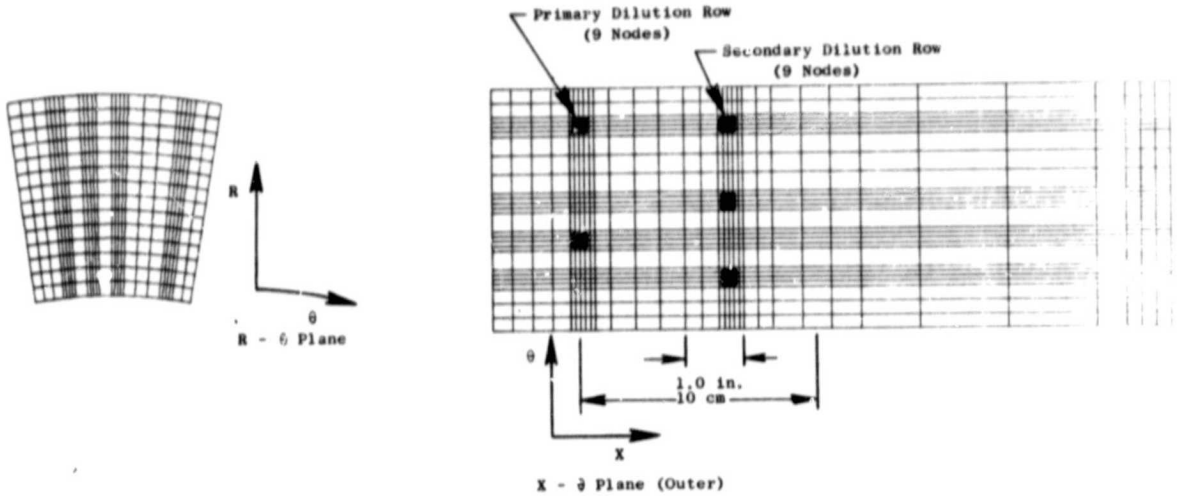

Figure 35. Coarse Grid Selected for Calculations of Experimental Test Configurations.

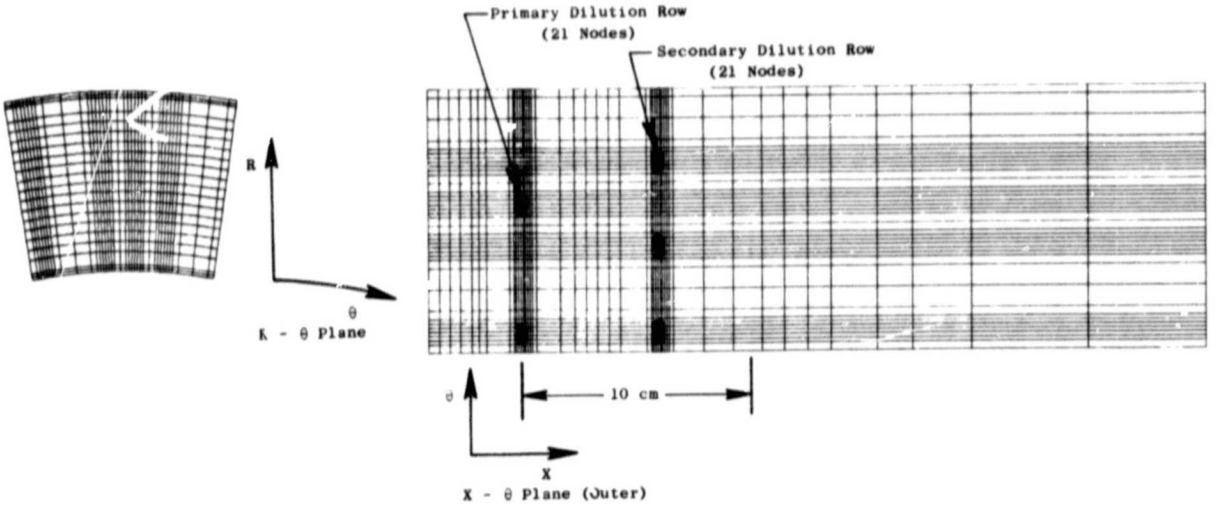

Figure 36. Detailed Grid Selected for Calculations of Experimental Test Configuration 17C.

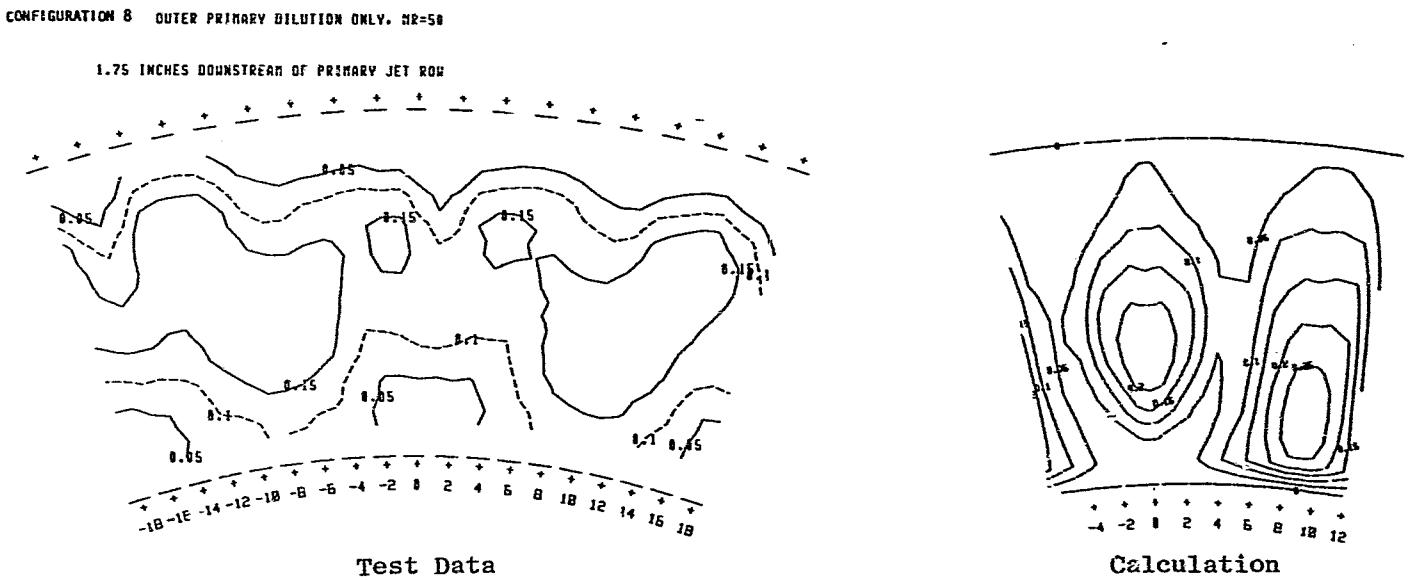

Test Data

Calculation

Figure 37. Comparison of Measured and Calculated Results for Experimental Test Configuration 8.

Contours of $\frac{T_{Inlet} - T_{Local}}{T_{Inlet} - T_{Jet}}$

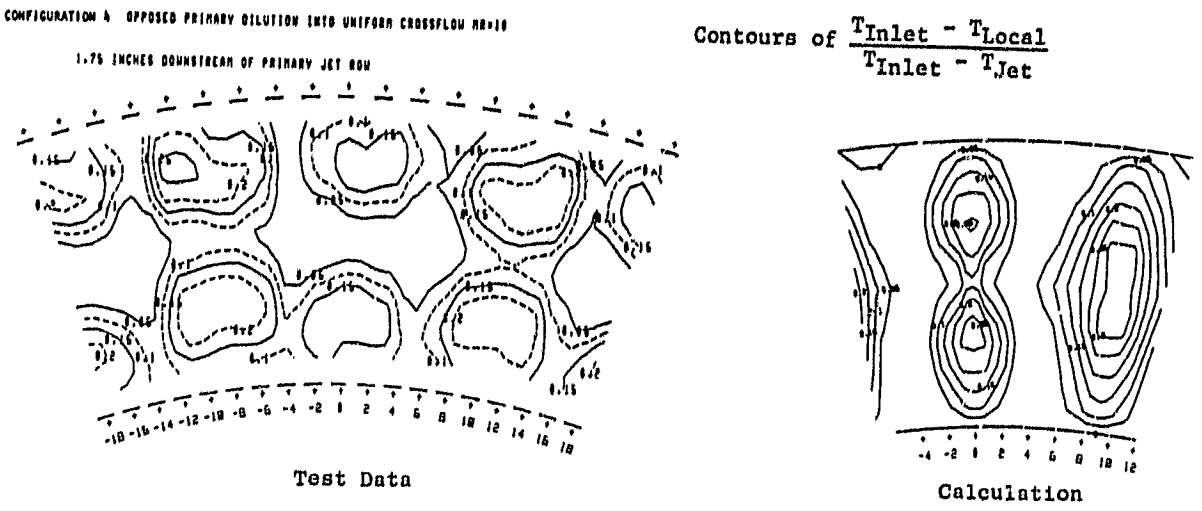

Figure 38. Comparison of Measured and Calculated Results for Experimental Configuration 4.

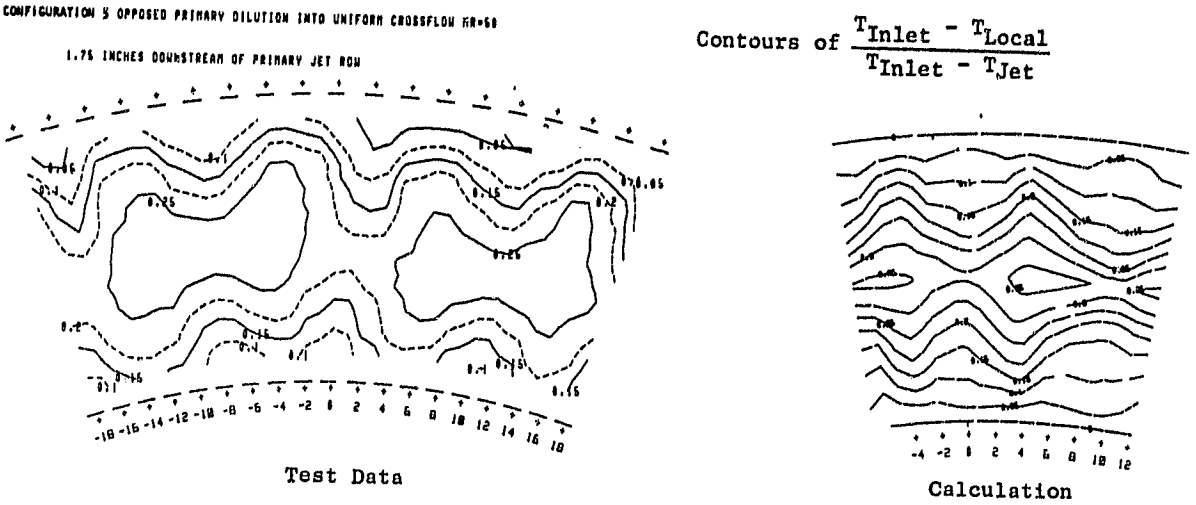

Figure 39. Comparison of Measured and Calculated Results for Experimental Configuration 5.

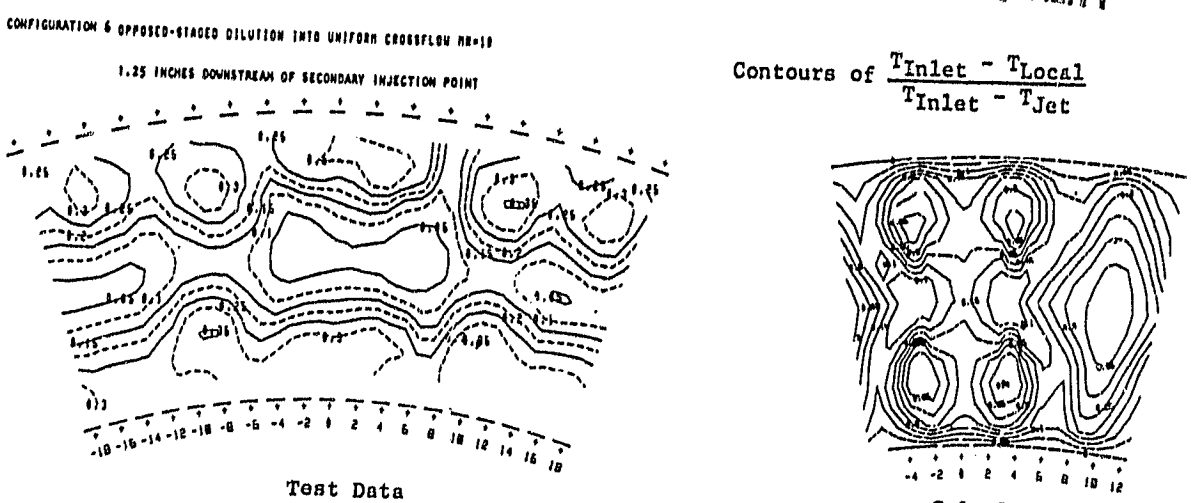

Figure 40. Comparison of Measured and Calculated Results for Experimental Configuration 6.

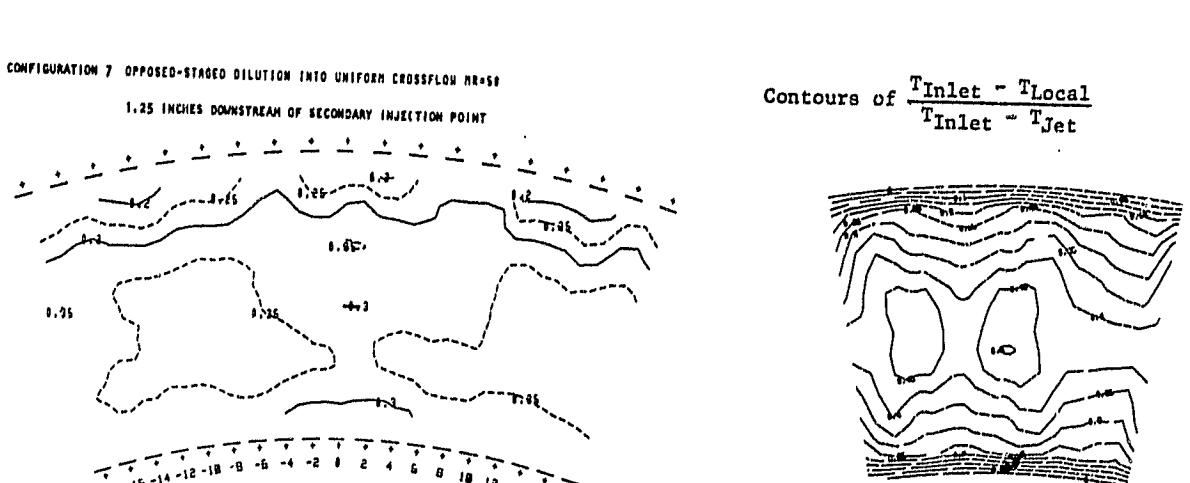

Figure 41. Comparison of Measured and Calculated Results for Experimental Configuration 7.

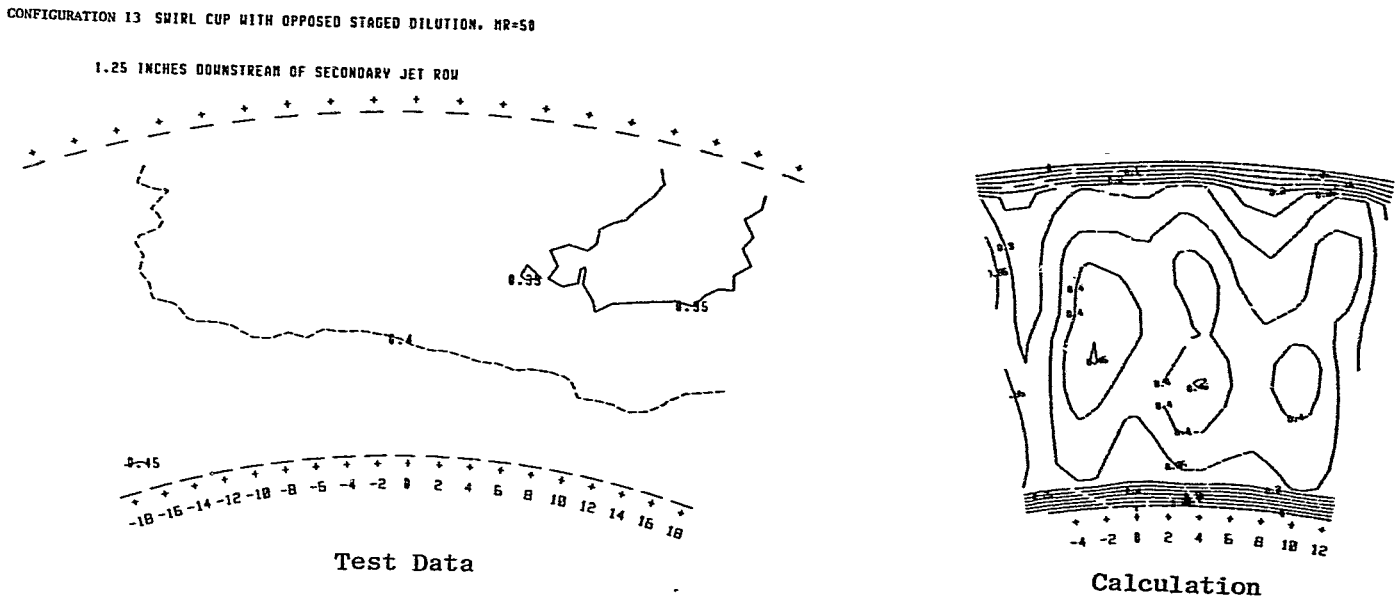

Figure 42. Comparison of Measured and Calculated Results for Experimental Test Configuration 13.

Contours of $\frac{T_{Inlet} - T_{Local}}{T_{Inlet} - T_{Jet}}$

INTFLOW Calculation

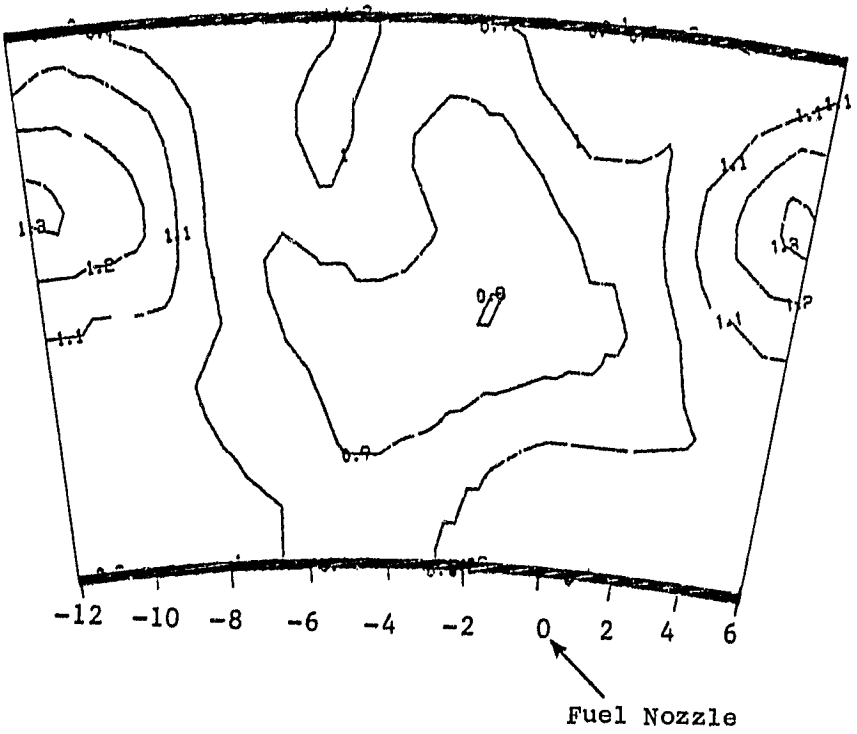

Sector Measurements

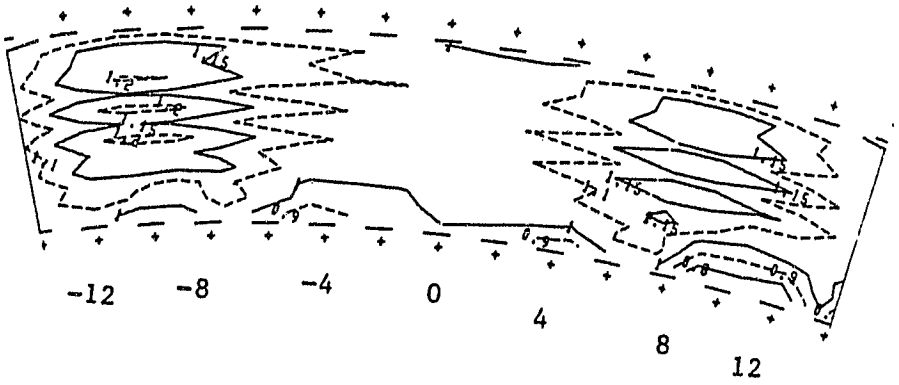

Figure 43. Comparison of Measured from Contoured Sector with INTFLOW Calculations Using Cylindrical Wall Grid (Liquid Fuel Injection).

inherent in the current 3-D codes where all Peclet numbers exceed 2.0 are needed. This would improve accuracy without requiring large increases in grid. The numerics must also feature faster convergence rates. Improvements in computation time is also an important consideration in making these codes more useful as design tools.

A true combustor has significant contour in the flowpath walls. The ability to utilize noncylindrical combustor walls using the stairstep technique was briefly explored. While the technique was described in the user's manuals available with the 3-D codes, and some of the framework was incorporated into the programming, it was not fully implemented. Near the end of this contract effort, modifications were introduced at General Electric through an ongoing IR&D program to permit the use of the stairstep technique. The GE/F101 combustor geometry with the grid shown in Figure 44, resulted in the calculated flow field shown in Figure 45. This example illustrates the significant waste of grid, using the rectangular grid system, required in the current 3-D codes. Approximately half the nodes lie external to the flowfield, and grid concentration near the walls for modeling film cooling features is very awkward. A body-fitted coordinate system would be beneficial for eliminating the deficiencies of the stairstep technique.

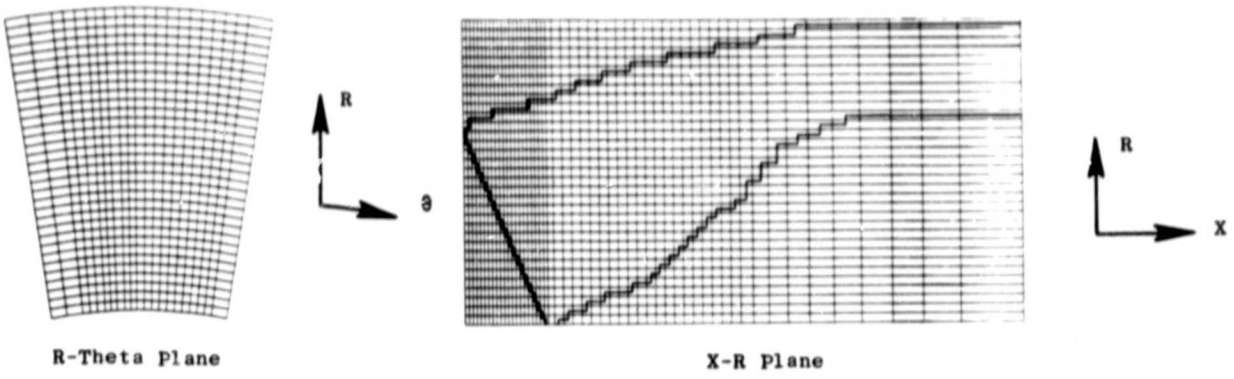

Figure 44. F101 Contoured Wall Grid (53X 34Y 23Z).

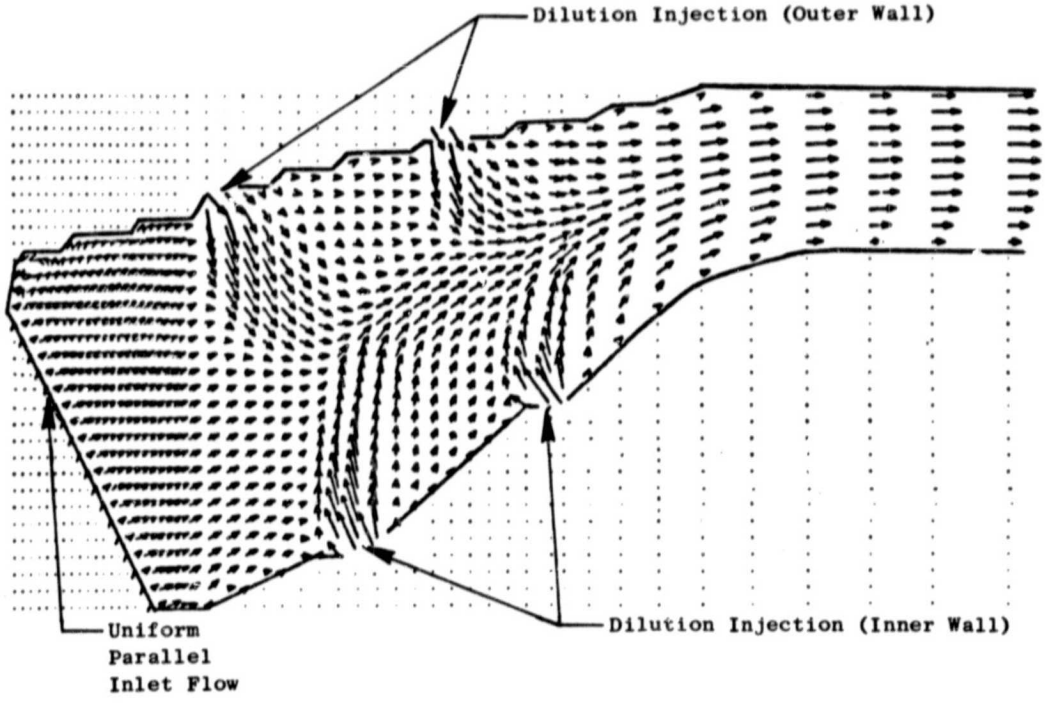

Figure 45. Combustor Calculation with Uniform Inlet (No Fuel).

IX. CONCLUDING REMARKS

For comparison with the aerothermal model, data were selected from General Electric's data base and from the literature and new experimental data were obtained. The new experimental data involved temperature distribution data from a series of combustor-like flows of progressively increasing flow complexity. Comparisons of modules within General Electric's overall aerothermal model were conducted.

The comparisons showed that the modules already in use are reasonably accurate. The principal weakness in the Heat Transfer Module is in the accuracy of the hot gas side input. Also, the currently used methods do not include a module for accurate analytical estimation of the combustor exit gas temperature.

The mathematical and physical bases of the internal flow module were investigated in one- and two-dimensional studies of various flows for which "benchmark" quality data were available. These studies addressed the "numerical diffusion" error due to the use of first-order accurate discretization schemes as well as the turbulence and turbulence-chemistry interaction phenomena.

The one-dimensional prescribed uniform velocity convection-diffusion equation was studied with and without source terms to ascertain the performance of various difference operators applied to the convection term; diffusivity was taken as a known constant. As is well known, differencing of the odd derivative can lead to instability if central differencing is used when the grid is coarse (local Peclet number greater than two). One-sided upwind differencing provides an unconditionally stable finite difference representation of the convection term but is accurate only to first order in the grid spacing. This is one order less accurate than the centrally-differenced diffusion term (which, being an even derivative does not have the stability problem) and leads to artificial diffusion. Thus, the convection term differencing operator must compromise between formal accuracy and stability. One-dimensional prescribed nonuniform velocity flows and two-dimensional uniform velocity flows were also modeled. All these studies indicated the need for a second-order scheme e.g., second-order upwinding or QUICK, rather than a first-order scheme, e.g., skew first-order upwinding which recognizes grid to streamline skewness but is still overly diffusive. Direct central-differencing of the convection term in three-dimensional flows is precluded by the excessive grid needed to ensure local Peclet numbers below two.

In the assessment of the physical submodels in two-dimensional recirculating flows, however, the grid density was increased until local Peclet numbers allowed central differencing. Such numerical error as existed was quantified. With this sound numerical basis the model was applied to three recirculating flows. A parabolic formulation - for which the numerical issue is not relevant - was also used to simulate a non-premixed jet flame for which high

quality optical data were available. These studies indicated that the suggested advanced physical models are necessary. Specifically, a probabilistic treatment for the random compositional fluctuations which lead to nonlinear turbulence-chemistry interaction is required. Furthermore, the isotropic eddy viscosity k-ε model was shown to be inadequate for flows with strong swirl components; an algebraic simplification of the full Reynolds stress equations which retains the two-equation format was suggested and validated.

In utilizing the 3-D calculations in INTFLOW, difficulties were encountered in obtaining good comparisons with measurements of dilution jet penetration and mixing data. Variations of grid detail and input quantities to the calculations were examined to determine their effect on the solution. It was found that the higher momentum ratio jets. Calculations done on the same experimental test case using both of the 3-D codes within INTFLOW, showed that similar penetration and mixing were calculated, even though the local calculated turbulence levels were different. The comparison of calculations for the dilution jet experiments conducted at General Electric are close in character to the measurements but not good enough to be a useful design tool at this time.

This effort did not establish the grid density needed to adequately treat dilution jets. To stay within reasonable computing time and storage demands, it is not possible to calculate combustor dilution patterns accurately with the available codes. The grid requirements for future 3-D codes with improved numerics could not be determined in this work; studies conducted with a 3-D code having the desired numerics improvements will be required to make this determination.

Comparison of calculations with an experiment that included fuel injection and heat release and a combustor dilution pattern, showed that the calculated gross temperature pattern in the gas of the combustor exit had considerable similarity to the measured values. Further analytical and experimental study is still needed, however, to define an adequate method for defining the input for the initial fuel and air distribution.

The computer running time costs of obtaining reasonable converged solutions was very high; thus future modeling improvements should strive for faster convergence techniques to increase the size of the maximum affordable grid along with alternate numeric schemes to provide greater accuracy for whatever grid is adopted. For inputting the dome air and fuel injection details, more experimental knowledge of the early flow development is needed.

PRIORITIZED RECOMMENDATIONS

Table II presents a prioritized list of the main recommendations for treating the sources of error in the current three-dimensional elliptic internal flow code INTFLOW. The list includes two paths: needed basic capability and application to durability. The efforts in the second category should begin whenever it is decided that the needed basic capability is progressing

Table II. Prioritized Recommendations.

Needed Basic Capability

1. Improved 3-D Code Framework
   - Body-Fitted Coordinate System
   - Improved Numerical Scheme
   - Faster Convergence Speed
2. Improved Turbulence and Turbulence/Chemistry Treatment
   - ASM (Algebraic Stress Model)
   - One Scalar PDF
   - Alternate to Two-Equation Turbulence Model
3. Develop Treatment of Inlet Boundary Conditions: Dilution, Fuel, and Swirlers
   - Based on Empirical Data Including Extensive GE Data Base and New Experiments
4. Improved Chemical Kinetics Treatment Including Turbulent Compositional Fluctuations

Application to Durability

1. Liner Heat Transfer Inputs
   - Fuel and Swirler Air Insertion Treatment
   - Hot Gas Mixing With Film Cooling Air to Couple with Heat Transfer Model
   - Radiation Effects, to be Developed Later
2. Pattern Factor 3-D Design Tool
   - Perturbation Approach Recommended

fast enough to justify work on features to permit the application to the design/development guidance process. These recommendations are based on a methodical study of 2-D flows and model problems and also on a more pragmatic application of the available 3-D code.

The first substantial improvement in capability can come from revisions in the basic code framework. A body-fitted coordinate system would permit needed improvements in the accurate treatment of the boundary, allow desired grid concentration near the walls, more flexible treatment of film slot heights, elimination of grid points outside of the flow field with their computer storage demands, and increased accuracy for all varying grid sizes throughout the flow field. Methods of accomplishing a body-fitted coordinate can include a basic nonorthogonal coordinate framework without any transformation, or a basic coordinate transformation technqiue. The latter seems most attractive at present.

Improved numerics should be incorporated, particularly a technique that will improve on first order upwind differencing by extending regimes in which second-order accurate schemes can be applied. Several methods have been discussed, but further study and evaluation would be recommended before selecting the most appropriate technique.

Since computer running costs are a serious limitation, improved convergence speed is also needed. Convergence speed is affected somewhat by the numerics adopted, but solution algorithms should be adopted to give reduced running costs and, when larger computer storage becomes available, to permit increased grids. The present pressure-correction equation approach to handling continuity is another serious drawback in that it requires a staggered grid (with attendant increase in storage requirements) and also can slow down the convergence rate.

The second item in the needed basic capability list is improved turbulence and turbulence/chemistry interaction treatment. This may be of less overall impact than the first item, but at least the first two improvements recommended have been implemented in 2-D at General Electric. The algebraic stress model for dealing with the turbulence anisotropy in swirling flows has been demonstrated and deserves to be included as an algebraic correction to the turbulence model.

The pdf, probability density function, treatment of random compositional fluctuations has been thoroughly evaluated. It is far superior in the character of its fundamental physics to the eddy breakup model in the current 3-D programs. This change is a very worthwhile improvement.

An appropriate change to the basic two-equation turbulence model to handle all flow regimes has not been indentified. Reynolds stress transport equations and improved dissipation rate equations may be the only option. Time wise, such a solution may be a long way into the future.

The third item calls for improvement in the boundary flow input treatments. Inputs based on the physical geometry are not adequate. The flows

leave the entry regions at angles and with turbulence levels that are affected by small geometry features that are not directly treated by the models. Accurate inputs for these features must come from empirical data. An extensive data base exists at General Electric, but additional data will ultimately be needed, and methods of translating this empirical information into inputs to the model need to be developed. Detailed analysis with a 3-D model of the flow through a specific aperture has been considered as a technique for generating the inputs for the larger solution, but the basic need would still involve a significant new data base.

The last item in the list of needed basic capabilities is in improved chemical kinetics treatment. This will become particularly important if the same model is to be used for emissions or blowout calculations. For durability alone its impact is small and, therefore, has been placed far down the list. Expanded joint pdf methods have, however, been given considerable attention at General Electric. Development concepts are available.

On the application to durability, the two durability design needs of liner heat transfer inputs and pattern factor calculations are listed. For both, a method for fuel and swirler air insertion is needed. As in the third item above, this involves accumulation of new data as well as an accompanying analytical study on how to use the data.

The boundary between the film cooling protection and the hot gas side flows is not distinct. Temperature velocity and turbulence gradients are all present. However, similar techniques that would be used to introduce finer grid near the wall to calculate through the film can also be used to define "effective" hot gas side conditions at the film protection boundary. This will permit the use of existing wind tunnel data on the effect of film protection slots of different designs. This technique needs to be defined and programmed.

Methods of treating flame radiation can be developed at a later time. New data is being accumulated on flame radiation in ongoing programs and this data could be used in calibrating any future calculation methods. The final flame radiation calculations are expected to be a hybrid calculation not integrated with the INTFLOW iterations but utilizing the final flow field.

The exit gas temperature pattern factor design tool is conceived as a perturbation calculation at this time. While the absolute temperature pattern may not be accurate, much greater accuracy would be expected for the perturbation effect due to a change in dilution hole pattern. The tool would be developed initially along this principle.

X. REFERENCES

1. Mongia, H.C., et al., "Combustor Design Criteria Validation," USATL-TR-78--55A, 55B, 55C, February 1979.

2. "The Design and Development of Gas Turbine Combustors Phase II Basic Computing System." Volume Report No. 1420, Northern Research and Engineering Corporation.

3. Claus, R.W., "Analytical Calculation of a Single Jet in Crossflow and Comparison With Experiment," National Aeronautics and Space Administration, Technical Memorandum 83027, 1983.

4. Lapp, M., Drake, M.C., Penney, C.M., Pitz, R.W., and Correa, S.M., "Turbulent $CO/H_2/N_2$ Jet Diffusion Flame in Coflowing Air," DoE Contract Report DE-AC04--78 ET 13146, 1983.

5. Green, A. and Whitelaw, J.H., "Measurements and Calculations of the Isothermal Flow in Axisymmetric Models of Combustor Geometries," J. Mech. Eng. Sci., 22, 119, 1980.

6. Vu, B.T. and Gouldin, F.C., "Flow Measurements in a Model Swirl Combustor." AIAA Paper No. 80-007, 1980.

7. Lightman, A.J., Richmond, R.D., Magill, P.D., Krishnamurthy, L., Roquemore, W.M., Bradley, R.P., Stutrud, J.S., and Reeves, C.M., "Velocity Measurements in a Bluff-Body Diffusion Flame," AIAA Fifteenth Thermophysics Conference, Snowmass, Colorado, AIAA-80-1544, 1980.

8. Walker, R. E. and Kors, D.L. "Multiple Jet Study Final Report," NASA CR1217, June 1973.

9. Holdeman, J. D. and Walker, R.E., "Mixing of a Row of Jets with a Confined Crossflow," AIAA 15, 243, 1977.

10. Ferguson, D.R. and Keith, J.S., "Modifications to the Streamline Curvature Program," NAS CR-132705, June 1975.